University of Padova
Department of Industrial Engineering DII
Faculty of Energy Engineering

Master thesis

Design and assessment of the exhaust channel to install a small wind turbine and power output evaluation of Air 30 wind turbine

Supervisor:

Prof. Ing. Giorgio Pavesi (University of Padova)

Co-supervisors:

Prof. Dr-. Ing Dieter Brillert (University of Duisburg-Essen)

Dr.-Ing. Bastian Dolle (Siemens Energy)

Candidate

Armin Minaei – 2050914

Academic year

2023 - 2024

b

Acknowledgment

I would like to express my deepest appreciation to my academic supervisors, Prof. Giorgio Pavesi and Prof. Dieter Brillert for providing me the opportunity to undertake the thesis work at the university of Duisburg-Essen.

Additionally, I extremely grateful to Dr.-Ing. Bastian Dolle and Dr.-Ing Sebastian Schuster for his intangible support, patience and guidance throughout the entire journey of my thesis.

I would also extend my sincere thanks to all the colleagues at the chair of turbomachinery for their generous support, kindness. This endeavor would not have been possible without their Point of view and insight which were truly helpful in achieving the project's targets.

I hold a deep sense of gratitude towards my family for their steadfast support, affection, and confidence in my capabilities. Their comprehension during the toughest stages of this journey has been a continual pillar of strength.

To my friends, who offered emotional backing, motivation, and empathy throughout this scholarly pursuit, I express my sincere appreciation.

To each individual who has played a part in this academic accomplishment, my gratitude is immense. Your assistance has been priceless, and for that, I am deeply thankful.

Padova, March 2024

armin minaei

Armin Minaei

d

Abstract

The Chair of Turbomachinery at the University of Duisburg-Essen recognizes the importance of training students in the design of wind turbines. As part of this effort, a wind turbine test facility will be set up in the laboratory of the department of mechanical engineering. This facility will house a test turbine from one of the most renowned manufacturers of micro to small scale wind turbines, namely Primus wind power or Ryse Energy, in the exhaust channel of an axial compressor.

A preliminary Computational Fluid Dynamics (CFD) study is required to ensure optimal test conditions. The aim of this study is to determine the best installation position in the space following the exhaust channel and to figure out the flow behavior. A CFD setup will also be developed for preliminary numerical performance calculations.

In this work, three different mass flow rates of 14.6, 11.3 and 8 kg/s are evaluated to determine the velocity values and homogeneity of the flow within the room. Additionally, in order to improve the velocity values within the designated room and also the homogeneity of the flow, the effect of installation of one honey comb has been assessed. The honeycomb which consists of two parts, flow domain and porous domain, has the same diameter of the hole inside the internal wall and three different porosities (0%, 40%, 70%) has been analyzed.

The next part of this thesis focuses on the Air 30 wind turbine as a small-scale wind turbine. The blade has been 3D scanned and a hub and pocket and ambient have been designed using Creo Parametric and therefore by modelling with Ansys tools such as ICEM to mesh, CFX to define the flow conditions and finally CFD-post processing to visualize the result. The main goal of this method is to determine the power output and power coefficients at various wind speeds.

The optimal location for the wind turbine is less than 80 cm from the wall to capture the maximum power output. The derived power versus wind speed graph closely matches the graph provided by the manufacturer.

f

Sommario

La Cattedra di Turbomacchine dell'Università di Duisburg-Essen riconosce l'importanza di formare gli studenti nella progettazione di turbine eoliche. Come parte di questo sforzo, sarà allestito un laboratorio per il test delle turbine eoliche nel laboratorio del dipartimento di ingegneria meccanica. Questo laboratorio ospiterà una turbina di prova di uno dei più rinomati produttori di turbine eoliche di piccola e micro scala, ovvero Primus Wind Power o Ryse Energy, nel canale di scarico di un compressore assiale.

È necessario uno studio preliminare di Fluidodinamica Computazionale (CFD) per garantire condizioni di test ottimali. L'obiettivo di questo studio è determinare la migliore posizione di installazione nello spazio a seguito del canale di scarico e capire il comportamento del flusso. Sarà inoltre sviluppato un setup CFD per calcoli di prestazioni numeriche preliminari.

In questo lavoro, vengono valutati tre diversi flussi massici di 14.6, 11.3 e 8 kg/s per determinare i valori di velocità e l'omogeneità del flusso all'interno della stanza. Inoltre, al fine di migliorare i valori di velocità all'interno della stanza designata e anche l'omogeneità del flusso, è stato valutato l'effetto dell'installazione di un pannello a nido d'ape. Il pannello a nido d'ape, che consiste in due parti, dominio del flusso e dominio poroso, ha lo stesso diametro del foro all'interno della parete interna e sono state analizzate tre diverse porosità (0%, 40%, 70%).

La parte successiva di questa tesi si concentra sulla turbina eolica Air 30 come turbina eolica di piccola scala. La pala è stata scannerizzata in 3D e un mozzo, una tasca e un ambiente sono stati progettati utilizzando Creo Parametric e quindi modellati con strumenti Ansys come ICEM per la mesh, CFX per definire le condizioni di flusso e infine il post-processing CFD per visualizzare il risultato. L'obiettivo principale di questo metodo è determinare la potenza di uscita e i coefficienti di potenza a varie velocità del vento.

La posizione ottimale per la turbina eolica è a meno di 80 cm dal muro per catturare la massima potenza di uscita. Il grafico derivato della potenza rispetto alla velocità del vento corrisponde strettamente al grafico fornito dal produttore.

h

Zusammenfassung

Der Lehrstuhl für Turbomaschinen an der Universität Duisburg-Essen erkennt die Bedeutung der Ausbildung von Studenten in der Gestaltung von Windturbinen an. Als Teil dieser Bemühungen wird eine Testeinrichtung für Windturbinen im Labor der Fakultät für Maschinenbau eingerichtet. Diese Einrichtung wird eine Testturbine von einem der renommiertesten Hersteller von Mikro- bis Kleinwindturbinen, nämlich Primus Wind Power oder Ryse Energy, im Auspuffkanal eines Axialkompressors beherbergen.

Eine vorläufige Studie zur Computational Fluid Dynamics (CFD) ist erforderlich, um optimale Testbedingungen zu gewährleisten. Ziel dieser Studie ist es, die beste Installationsposition im Raum nach dem Auspuffkanal zu bestimmen und das Strömungsverhalten zu ermitteln.

Ein CFD-Setup wird auch für vorläufige numerische Leistungsberechnungen entwickelt. In dieser Arbeit werden drei verschiedene Massenströme von 14,6, 11,3 und 8 kg/s bewertet, um die Geschwindigkeitswerte und die Homogenität der Strömung im Raum zu bestimmen. Zusätzlich wird zur Verbesserung der Geschwindigkeitswerte im vorgesehenen Raum und der Homogenität der Strömung die Wirkung der Installation eines Wabenkammes bewertet. Der Wabenkamm, der aus zwei Teilen besteht, dem Strömungsdomäne und dem porösen Domäne, hat den gleichen Durchmesser des Lochs in der Innenwand und drei verschiedene Porositäten (0%, 40%, 70%) wurden analysiert.

Der nächste Teil dieser Arbeit konzentriert sich auf die Windturbine Air 30 als Kleinwindturbine. Die Klinge wurde 3D-gescannt und ein Naben- und Taschen- und Umgebungsmodell wurde mit Creo Parametric erstellt und dann mit Ansys-Tools wie ICEM zur Netzgenerierung, CFX zur Definition der Strömungsbedingungen und schließlich CFD-Postprocessing zur Visualisierung des Ergebnisses modelliert. Das Hauptziel dieser Methode ist es, die Leistungsausgabe und Leistungskoeffizienten bei verschiedenen Windgeschwindigkeiten zu bestimmen.

Die optimale Position für die Windturbine ist weniger als 80 cm von der Wand entfernt, um die maximale Leistungsausgabe zu erfassen. Das abgeleitete Diagramm der Leistung im Vergleich zur Windgeschwindigkeit stimmt eng mit dem vom Hersteller bereitgestellten Diagramm überein.

j

Table of content

m

List of figures

List of tables

p

1. Introduction

The world is currently facing an energy crisis. With the increasing demand for energy and the need to reduce environmental pollution, it is imperative to explore alternative sources of energy. One such promising source is wind power, which is renewable, abundant, and environmentally friendly. This thesis focuses on the design and optimization of wind turbines, a critical component of harnessing wind power.

The Chair of Turbomachinery at the University of Duisburg-Essen recognizes the importance of educating students in the design of modern, high-efficiency wind turbines. As part of this initiative, a test facility for blade testing will be installed in the laboratory of the chair of turbomachinery in the department of mechanical engineering. This facility will feature a test turbine situated in the exhaust channel of an axial compressor, providing an adjustable airflow rate for the making reasonable to install a small wind turbine. The small wind turbine which is supposed to install in this room has been purchased from a manufacturer called Prisms Wind Power (Ryse Energy).

However, to ensure optimal testing conditions, a preliminary Computational Fluid Dynamics (CFD) study is necessary. This study aims to identify the optimal installation position in the exhaust channel and arrangements for flow conditioning. Additionally, a CFD setup for rapid preliminary numerical performance calculations will be composed.

This thesis is divided into several working parts. The first involves the generation of a three-dimensional numerical domain of the exhaust channel. Subsequent part includes running numerical calculations of the exhaust channel with modified arrangements for flow conditioning such as different mass flow rate of the flow exiting the axial compressor and entering the exhaust channel, implementing a domain for turbine simulation.

The objective of this thesis is to identify the most suitable location for installing the wind turbine. This will be achieved by examining various analysis of the flow within the room, both without an internal wall and also with defining a wall with a hole in the center exactly after the silencer, and additionally incorporating a honeycomb structure to create a jet and further homogenize the flow and assessing the impact of different values of porosities (without porosity, 40% and 70%). The main goal of the analysis is to find the reliable data of velocity and its homogeneity in different locations within the room and finally the best location to install the small wind turbine.

In this study, an Air30 wind turbine blade was 3D scanned by an expert company in Duisburg, Germany. The blade was coupled with a hub inside Creo Parametric software. To assess the wind turbine's characteristics, two control volumes were designed in the software, meshed using the Ansys ICEM tool, and boundary conditions were defined in Ansys CFX.

Introduction

Finally, through assessment and analysis in CFD post-processing, values such as power and torque that can be extracted from it were calculated.

2. Fundamentals

2.1.　　Wind energy

The history of wind energy is long and fascinating. It dates back to ancient civilizations. In Egypt, where sails were used to navigate the Nile River, the earliest evidence of wind power can be found around 5000 BC. The idea of harnessing wind for mechanical power is thought to have been conceived in ancient Babylonia, with plans to use wind power for irrigation projects in the seventeenth century BC.

During the Middle Ages, wind power was used extensively in Europe. Windmills, known as 'tower mills', became a common sight in rural landscapes and were used for a variety of purposes, including grain milling, oil production and textile processing. The industrial era of the 19th century brought significant advances in wind power technology. The introduction of metal blades improved the efficiency and durability of windmills, which were then used to power industrial machinery such as sawmills, foundries and paper mills.

In the 20th century, the focus shifted to using wind energy to generate electricity. The first electricity-generating wind turbine was installed by Josef Friedländer at the Vienna International Electrical Exhibition in 1883. However, it was the 1973 oil crisis and growing environmental awareness that really promoted wind as an alternative to conventional energy.

Today, wind power is mainly generated by wind turbines. These are often grouped together in wind farms and connected to the electricity grid. In 2022, wind power supplied over 2000 TWh of electricity, accounting for over 7% of global electricity.

In recent years, the discourse has evolved to go beyond simply promoting windmills. The detrimental impact of fossil fuel use, which is predicted to increase the Earth's temperature by 2.7°C by the end of the century[1]., has necessitated a shift towards renewable energy sources. Wind energy has emerged as one of the leading renewable energies and represents a crucial step in our collective efforts to combat climate change and promote sustainable development.

Global energy use has increased remarkably for decades. Many developing countries have made substantial efforts to minimize the climate change impacts by optimizing energy use[2]. The extensive burning of fossil fuels releases large amounts of greenhouse gases, including CO_2 and CO, exacerbating global warming and climate change. Fossil fuel energy generation is only 30-40% efficient, leading to over half of the energy being wasted as heat, negatively affecting both the economy and environment.

Global energy-related CO_2 emissions grew by 0.9% or 321 Mt in 2022, reaching a new high of over 36.8 Gt, due to specific challenges in 2022 that contributed to the growth in

emissions, although CO2 growth in 2022 was well below global GDP growth of 3.2%. Nowadays, due to the rising need for energy, it is urgent to find alternatives to fossil fuels to decrease their use and reduce greenhouse gas emissions. A strong expansion of renewables, which met 90% of last year's global growth in electricity generation, with solar PV and wind generation each increasing by around 275 TWh, a new annual record, limited the rebound in coal power emissions.[3]

Figure 2-1 illustrates various types of global energy production from 2010, with projected values up to 2027. Wind and solar energy display a significant upward trend, expected to reach 1500 GW and approximately 2700 GW, respectively in the next four years. Natural gas, coal, and bioenergy also show an upward trend, but their growth rate is predicted to slow down in the coming years.[4]
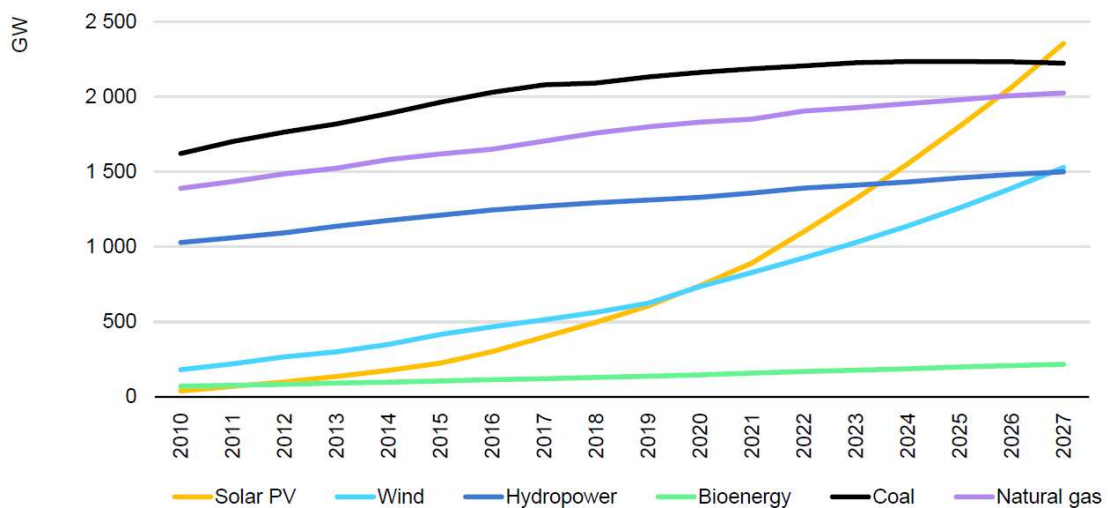
Figure 2-1 Cumulative power capacity by technology, 2010-2027 [4]

In Figure 2-2 the progression of wind electricity capacity over the years 2022, 2023, and 2024 is depicted. It is evident from the data that China has demonstrated a significant commitment to this form of renewable energy. Unlike other regions, China has consistently maintained its wind electricity capacity at an impressive level of approximately 60 GW.
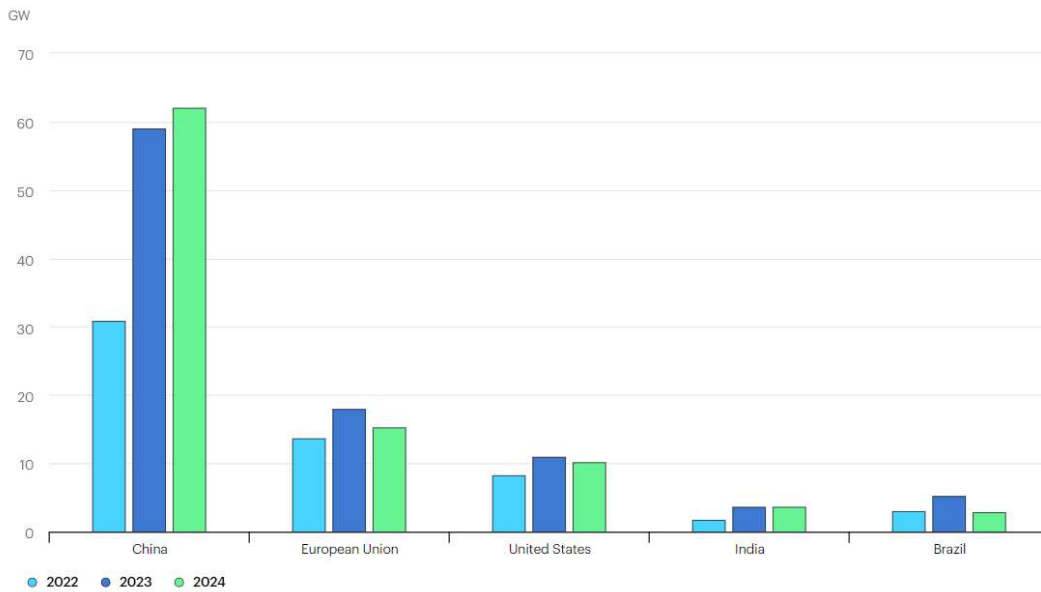
Figure 2-2 Net onshore wind electricity capacity addition by country or region [4]

Wind energy derives from the kinetic energy of moving air, also known as wind. This wind is created when the sun heats the Earth's surface unequally, causing air to flow from high-pressure areas to low-pressure areas. Wind turbines capture this kinetic energy from the wind and turn it into mechanical power. This mechanical power is then converted into electrical power. In order to extract the energy from wind, there are two main types of wind turbines which will be explained in the following sections. Additionally, small wind turbines and its own characteristics will be elaborated in detail, which is the main focus of this work.

2.2. Wind turbines

Wind turbines are mainly classified into two main types depending on the axis of their own rotation called horizontal and vertical wind turbines.

2.2.1. Horizontal axis wind turbine

A wind turbine is the main device used to convert wind energy into electricity. It consists of substantial parts, such as the tower, rotor, nacelle, and blades. The tower holds up the turbine and lifts it high enough to interact with high wind speeds. The rotor, which includes the hub and blades, captures the wind and turns its energy into spinning motion. The nacelle is like a little house for the important parts of the turbine, like the gearbox, generator, and control systems. In Figure 2-3 the main components of horizontal wind turbines is

illustrated.[5]
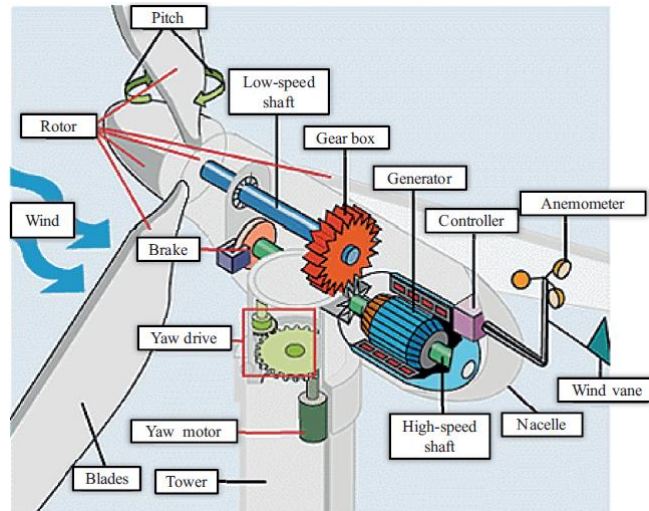
Figure 2-3 Horizontal wind turbine components [5]

In the horizontal axis wind turbine, rotor, shaft and blades are aligned horizontally which makes them more efficient in high wind speed regions and mainly in large-scale on-shore and off-shore wind farms. Wind turbines can be installed on the land classified in on-shore wind turbines or in the waters such as lakes, oceans named off-shore wind turbines. The advantages of on-shore wind turbines compared to offshore turbines include cost effectiveness, quicker installation and easier maintenance, and less environmental impact. On the other hand, this type of wind turbines has its own disadvantages. These include intermittent generation of electricity, the noise produced by the wind farm which can affect people and nature, and aesthetic concerns raised by people. Additionally, onshore wind turbines generally have a lower power output, with an average onshore wind turbine producing around 2.5 to 3 megawatts (MW), compared to the offshore average of 3.6 MW.

At present, horizontal-axis wind turbines (HAWTs) are the most popular among all windmill designs. This is primarily because HAWTs generally have much higher efficiency than VAWTs. The maximum mechanical efficiency of a modern HAWT has been reported to be up to 45% to 50% while that of an efficient VAWT normally lies below 40% [6] (mechanical efficiency of a Savonius-type VAWT is even lower, normally below 25% [7])

2.2.2. Vertical axis wind turbine

Most early wind turbines were of vertical-axis type because they were relatively simple to construct (especially for milling) and did not require any mechanism to orient themselves towards the direction of the wind. In spite of these attributes, none of the old designs survived to the present day. Currently, there are three popular VAWT designs: (a) Savonius,

(b) Curved-blade Darrieus, and (c) Straight-blade Darrieus, as shown in Figure 2-4.
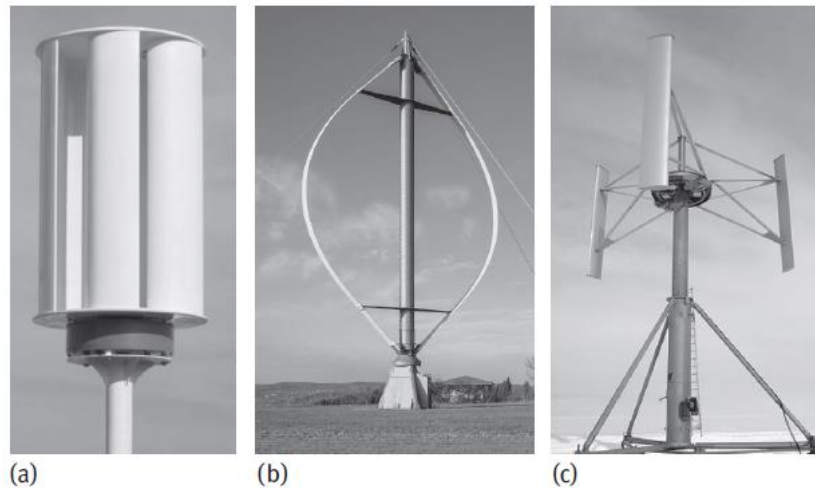
Figure 2-4 Vertical axis wind turbines. (a) Savonius rotor, (b) Curved-blade Darrieus rotor, (c) Straight-blade Darrieus rotor [8]

In principle, Savonius rotors normally have two opposing cups or half-cups on a central shaft, as shown in Figure 2-4a. The drum facing the wind stream captures the wind and generates a moment along the axis. The aerodynamic torque generated by the first drum causes the rotor to rotate and brings the drum on the opposite side against the wind flow. The second drum now catches the wind and causes the rotor to rotate even further, thus completing a full revolution of the rotor. This process continues until there is enough wind to turn the axial shaft, usually connected to a pump or generator.[9]

Savonius turbines, while generally having a low efficiency (<25%), making their commercial viability limited compared with HWTs, have advantages for low power applications: simple construction with low costs, high startup and dynamic torque, able to capture the wind regardless of directions, low noise and angular velocity in use, and reduced wear on moving parts.[7]

The VAWTs of the Darrieus type are made up of two or more blades that are attached to a vertical central shaft. These blades can be curved or straight, as shown in Figure 2-4. Regardless of curvature, the blades have an airfoil profile that creates aerodynamic lift when exposed to wind. This phenomenon creates a torque around the axis and causes the central shaft to rotate, ultimately turning the generator to produce electricity. The curved-blade Darrieus VAWTs have less bending stress in the blades than the straight-blade Darrieus VAWTs and are therefore more commercially successful [9]. However, for small-scale power generation, the straight-bladed Darrieus VAWTs are more popular due to the simplicity of the blade design [7]. It has been found that constant pitch straight-bladed Darrieus VAWTs cannot self-start [10], so straight-bladed Darrieus VAWTs may feature a variable pitch angle. Although this allows the turbines to overcome the starting torque

problem, it also complicates their design, making them quite impractical for small-scale power generation [9].

2.3.   Applying Blade Element Momentum theory (BEM) to small wind turbine blade design

The five crucial parameters influencing the power coefficient of the wind turbines are: (1) the airfoil design, (2) the angle of twist, (3) the length of the chord, (4) the tapering angle, and (5) the number of blades. In order to maximize the power coefficient, it is essential to optimize each of these parameters.

2.3.1. Iterative scheme for BEM theory

While the formulation of BEM is straightforward, an iterative method is required in order to implement the practical design of wind turbines. method. This is due to the implicit relationship between the blade parameters such as twist angle and chord length, operating conditions such as wind speed and rotor rotational speed, and the induction factors a and a'.

The main steps of one of the iterative schemes that can be used to design an SSWT are given below:

(a) Divide the blades into 15‑20 span-wise differential blade elements,
(b) Select a differential blade element i at radius r and thickness dr,
(c) Start with some guesstimate values for a and a' (e.g., a = 0 and $a' = 0$),
(d) Calculate relative wind speed and relative inflow angle using the following equations:

$$u_{rel} = \sqrt{[(1 - a)u_\infty]^2 + [(1 + a')\omega r]^2} \qquad (2.1)$$

$$\phi = \frac{(1 - a)u_\infty}{(1 + a')\omega r} \qquad (2.2)$$

(e) Determining the angle of attack for the given local twist angle β using the given equation:

$$\alpha = \phi - \beta \qquad (2.3)$$

(f) Calculate the Reynolds number using the following equation:

$$Re = \frac{\rho c u_{rel}}{\mu} \qquad (2.4)$$

(g) Look up the values of lift and drag coefficients (C_L and C_D) in published literatures for a given airfoil at various Reynolds number and angle of attacks. For the Flat plate, fully stalled regime, use the following equations:

$$C_L = 2C_{L,max}sin\alpha cos\alpha \qquad (2.5)$$

$$C_D = 2C_{D,max}sin2\alpha \qquad (2.6)$$

Where:

$$C_{L,max} = C_L \ at \ \alpha = 45°$$

$$C_{D,max} = C_L \ at \ \alpha = 90°$$

(h) Calculate the blade loss factor using the following equations:

$$F_{tip} = \left(\frac{2}{\pi}\right) cos^{-1}[e^{-\frac{B(r_t-r)}{2rsin\phi}}] \qquad (2.7)$$

$$F_{hub} = \left(\frac{2}{\pi}\right) cos^{-1}[e^{-\frac{B(r-r_h)}{2r_hsin\phi}}] \qquad (2.8)$$

$$F = F_{tip} \times F_{hub} \qquad (2.9)$$

(i) Calculate the value of axial induction factor a using the following equation:

$$if \ a < 0.4 \ then \ a = \cfrac{1}{\left[1 + \cfrac{4Fsin^2\phi}{\cfrac{cB}{2\pi r}(C_Lcos\phi + C_Dsin\phi)}\right]} ; \qquad (2.10)$$

$$if \ a \geq 0.4 \ then \ a = \frac{18F - 20 - 3\sqrt{C_T(50 - 36F) + 12F(3F - 4)}}{36 \ F - 50}, \qquad (2.11)$$

Where C_T is the thrust coefficient and is given as:

$$C_T = \left(\frac{cB}{2\pi r}\right)\left(\frac{1 - a}{sin\phi}\right)^2 (C_Lcos\phi + C_Dsin\phi) \qquad (2.12)$$

(j)

$$a' = \cfrac{1}{\cfrac{4\,sin\phi cos\phi}{\sigma_r C_y} - 1}$$

(2.13)

Where chord solidity $\sigma_r = \frac{cB}{2\pi r}$ and $C_y = C_L sin\phi - C_D cos\phi$

(k) Repeat steps (d) to (j) until achieving the convergence.
(l) Repeat steps (c) to (k) for each of the differential blade elements.
(m) Add the differential power produced by all the differential blade elements to obtain the total wind power of the wind turbine.
(n) Calculate the power coefficient of the wind turbine using following equation:

$$C_p = \frac{8}{\lambda^2} \int_{\lambda_r}^{\lambda} Fsin^2\phi(cos\phi - \lambda_r sin\phi)(sin\phi + \lambda_r cos\phi)\left[1 - \left(\frac{C_D}{C_L}\right)cot\phi\right]\lambda_r^2\, d\lambda_r$$

(2.14)

2.3.2. Size of the wind turbine

In order to design a small-scale wind turbine, at least two pieces of information are necessary: first, the required power output and secondly, the average wind speed of the ambient where the turbine is installed. Therefore, the diameter D of the wind turbine is given by following equation:

$$D = \sqrt{\frac{8P}{\eta\rho u_\infty^3}}$$

(2.15)

The value of η represents the overall efficacy including generator and can be guessed in the range of 20-25% as an initial guess for a small-scale turbine.

2.3.3. Airfoil selection

One of the most important steps in designing an efficient SSWT is the selection of airfoil. The lift to drag ratio decreases drastically when Reynolds number decreases. Thus, correctly estimating the value of Reynolds number is crucial. In the formulation of Reynolds number, contains relative wind speed depending on many unknown variables in the first step such as chord length, ω angular velocity, induction factors a and a'. Each of these variables needs to be guessed correctly.

If tip speed ratio λ is known, rotation rate can be calculated by following equation:

$$\lambda = \frac{\omega r_t}{u_\infty} \qquad\qquad (2.16)$$

For large scale wind turbines, the optimal value of tip speed ratio is between 8 and 10, whereas for small-scale wind turbines suggested values lie in the range of 2 to 4 to lower the noise level and improve the reliability of performance.[11]

Tip speed ration can be initially guessed to be 3 and chord length can be assumed to be equal to 15% of the wind turbine rotor. After estimating the Reynolds number, the most important step is the selection of suitable airfoil which performs the best by the given Reynolds number. One of the favorable airfoils among researchers is NACA 0012 that has been widely investigated.[12]

2.3.4. Blade twist angle

It can be concluded from (2.2) that the relative inflow angle ϕ is inversely proportional to the radius of the wind turbine. In other word, the inflow angle is at its maximum at the hub and gradually decreases towards the tip. In order to optimize the performance, the blade of the wind turbine must be twisted, ensuring the consistent interact of the wind with the blades at the optimal angle. One of the most special features of SSWTs is that the blade is highly twisted near the hub. This large twist angle leads to generate high starting torque which helps the wind turbine rotor to start at low wind speeds.

Lanzafame et al [13] investigated 1W small scale wind turbine and found out at the angle of attack equal to 10, the twist angle near the tip would be negative. They discovered that the negative value of twist angle is not desirable and results in decreasing the power coefficient.

Figure 2-5 demonstrates the iterative scheme used to optimize and design the blade for a fixed wind speed called design wind speed.
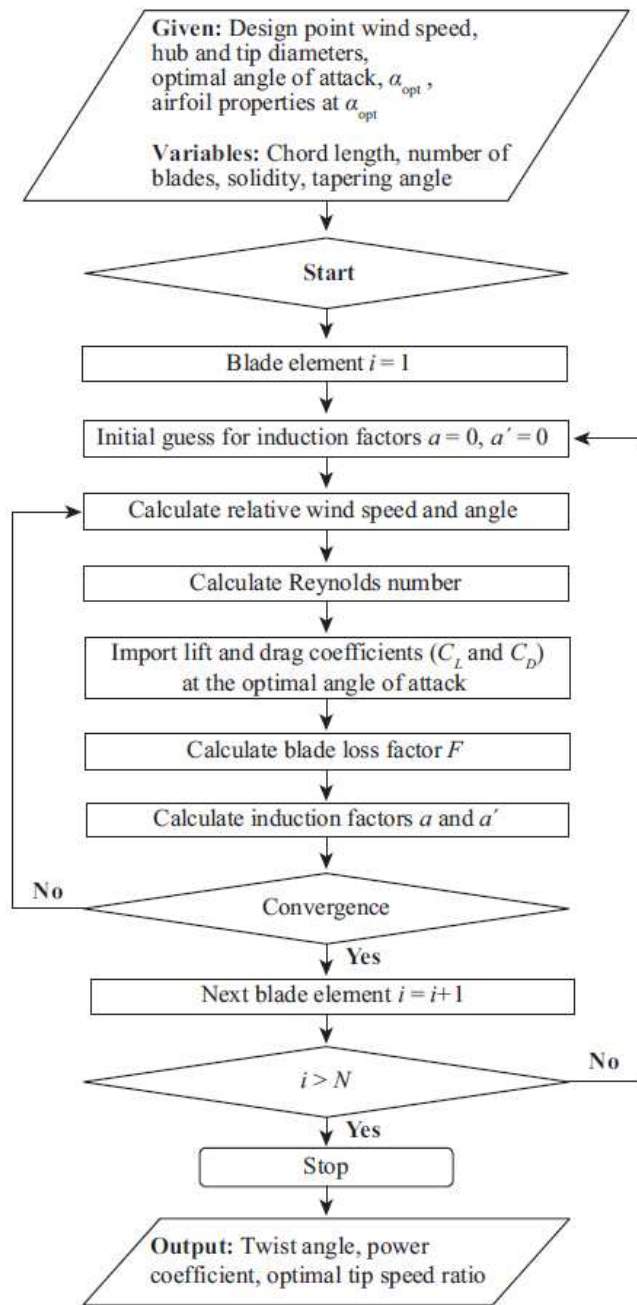
Figure 2-5 iterative scheme to optimize blade parameters at design wind speed

2.3.5. Wind turbine performance

In reality, the wind turbine does not operate only under its design operating condition. Consequently, it is necessary to have the tool and method to design wind turbine blades under off-design conditions.

In Figure 2-6 the iterative scheme to discover the power coefficient in different wind speeds is illustrated.
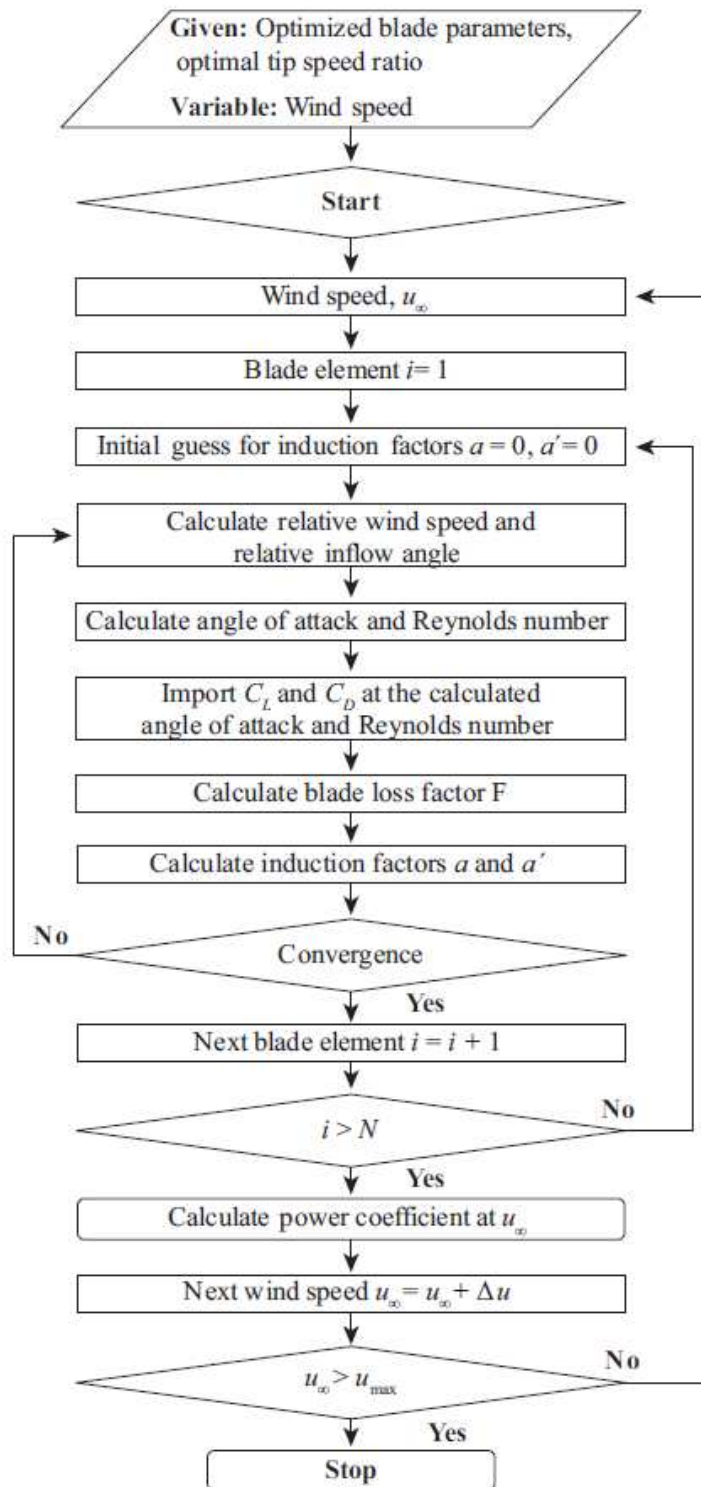
Figure 2-6 iterative scheme to predict power coefficient in different wind speeds

2.4.   Forces on wind turbines

In Figure 2-7 forces on a blade element of the wind turbine blade are illustrated. S stands for torque and T for thrust force, L and D represent lift and drag respectively and F is the overall force which is equal to the sum of lift and drag. ω represents the angular velocity of the wind turbine around its rotating axis and also the direction of wind speed and relative wind speed could be seen.
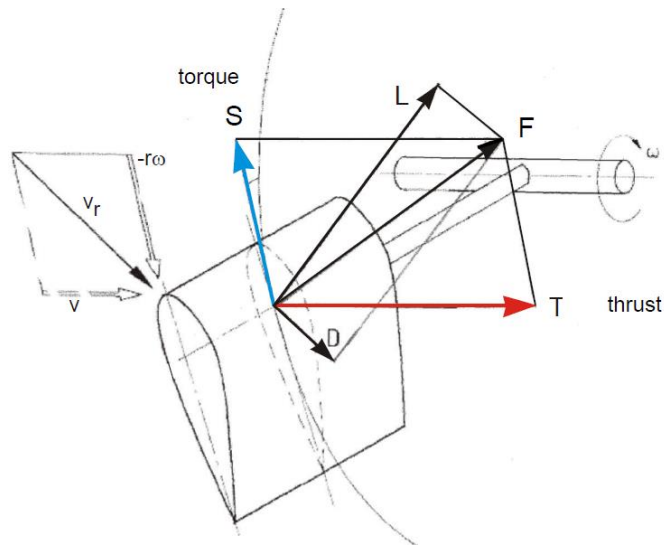
Figure 2-7 Forces on a blade element

In Figure 2-8 the lift and drag forces and its directions are depicted on an airfoil. In addition, the angle of attack is defined as the angle formed between the relative velocity and chord line, the line connecting the leading and trailing edge of the airfoil.
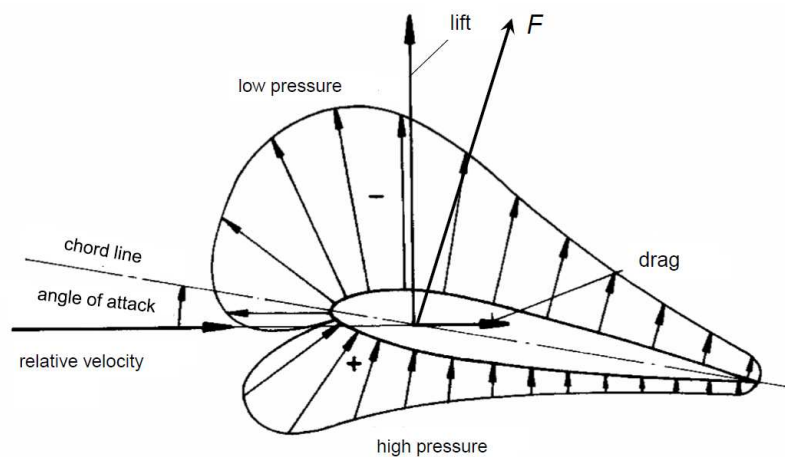
Figure 2-8 lift and drag on an airfoil

Due to the generated air pressure difference on the two sides of wind turbine blade, air

moves faster in the low-pressure side of the blade. Lift is the aerodynamic force exerted on an airfoil acting perpendicular to oncoming air flow. On the other hand, drag is the resistance experienced by the airfoil acting parallel to the wind direction.

2.5.   Ansys software

In this thesis, in order to carry out the performance of the wind turbine the package of Ansys software is used. This software due to the extensive variability of tools enables the user to model any geometry and discover the required parameters in the turbomachinery applications. One of the main benefits of Ansys package is that the whole procedure from creation the geometry until the demonstrating the results in different manners is possible in Ansys workbench and each step can be easily and directly managed. Moreover, in each section because of the different section tabs, it is much easier to change the parameters of the geometry, meshing or the boundary condition to make it much more similar to the realistic model. This tool also provides different type of simulations such as steady-state and transient. Additionally, Ansys can easily be adjusted with other tools, especially the tools which are focused on design and create a new geometry such as solid-edge, solid-work and PTC Creo parametric and other powerful tools. This characteristic of Ansys led to its widespread popularity among manufacturing companies. These companies utilize Ansys to analysis their geometry under various conditions, thereby identifying the weaknesses and strengthens of their design. This comprehensive analysis facilitates design improvements, ultimately to a point where the majority of engineers and experts agree to move on to the production stage of the designed model. This process underscores the main value of Ansys in the product development lifecycle.

Ansys workbench consists of wide variety of power tools which are even used in civil engineering and structural engineering. Here in this work, the main focus is on the parts which are usual for mechanical and particularly for turbomachinery investigations. In Figure 2-9 the usual work flow of Ansys is depicted.
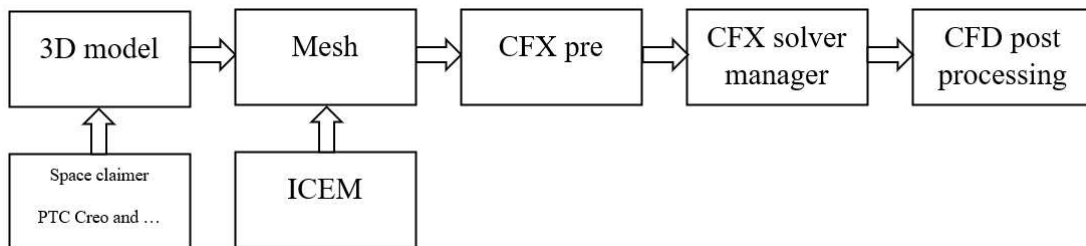
Figure 2-9 workflow of Ansys software

The initial phase is involving of the model's geometry. This can be accomplished in the Design Modeler or by importing from other software tools. The next phase involves meshing the geometry, which can be done in structured or unstructured forms to define tetrahedral and hexahedral meshes, respectively. This results in computational grid.

Once the mesh has been created, the simulation setup is follows in CFX. This setup involves defining the boundary conditions and define the different parts of the model such as inlet, outlet of the flow. It also involves informing the software know whether the model is stationary or rotating and flow characteristics or any other crucial factors that could influence the simulation outcome.

The output file of ICEM consists of .tin files which represents the model's geometry, and .blk and .uns for the structured and unstructured mesh, respectively. The output file of CFX is .def which is then used in CFX solver manager to define the run. This allows users to change the circumstances based on the characteristics of available system such as CPU and other main factors.

After achieving the convergence of the results in Solver Manager, the results are ready to be presented in CFD post processing tools. CFD-post enables the user to demonstrate the result in the most suitable way. Additionally, this tool provides a professional calculator which enables engineers to calculate the forces such as lift and drag on the desired locations and other characteristics like torque, thrust and power output. Apart from that creating animations to visually demonstrate how the flows and the model behave, making it more understandable for users.

3. Small wind turbines

The classification of wind turbines as "small" or "large" scale has been ambiguous in wind energy literature. Initially, small wind turbines were characterized based on its ability to generate enough electrical power to meet the required electricity needs by single households. The challenge, however, lies in the variability of the electricity consumption depending on the both geographical location and time. For instance, in order to fulfill the electricity demand of an average American family, a 10kW turbine would be required, whereas European household would require 4kW turbine and a Chinese equivalent household need only 1kW turbine.

In this work, the classification of wind turbines are based on the size of the horizontal-axis wind turbine rotors:[14]

    I.   Micro-scale wind turbines (μSWT): rotor diameter ≤ 10 cm,

    II.   Small-scale wind turbines (SSWT): 10 cm < rotor diameter ≤ 100 cm,

    III.   Mid-scale wind turbines (MSWT): 1 m < rotor diameter ≤ 5m, and

    IV.   Large-scale wind turbines (SSWT): rotor diameter > 5m.
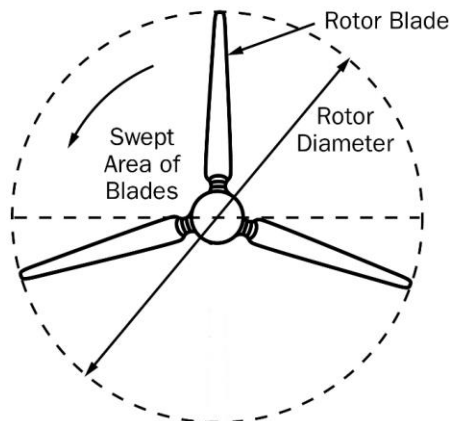
Figure 3-1 Rotor diameter and swept area of a wind turbine

The conventional large scale wind turbines (LSWTs) are efficient and the modern megawatt wind turbines have a power coefficient of up to 40-45% [15]. However, they require a high wind speed to operate; the typical rated wind speed is in the range of 12-14 m/s. Furthermore, due to practical concerns about safety hazards and noise emissions, their installation is limited to areas far from a city or town. In contrast, small-scale wind turbines (SSWTs) can operate at low wind speeds and produce minimal noise, and There are no known major safety hazards. The rated wind speed for mid-scale wind turbines is typically above 10 m/s.

In wind speed conditions below 5m/s, none of the wind turbines can operate efficiently

except the micro wind turbine. The micro-wind turbine, which operates in the range of 2-7 m/s, has an optimal power coefficient of 18%, which is quite low. The µF500 is the only SSWT that has a good overall efficiency value of 25%, but its rated wind speed is 12 m/s. The lack of suitable SSWT models that can operate near the ground in wind speeds of the order of a few meters per second is a major issue in the current state of SSWTs.

3.1. Air 30/40 land and marine wind turbines

Primus wind power [16] is a leading company in the production of small off-grid, hybrid system using small air wind turbines with advanced microprocessor smart controllers without mechanical break. The company's main products are Air 30 Turbine, Air Max, Air Silent X, Air 40 Turbine, Air X Marine Turbine and Air Breeze Turbine. These products have the same characteristics of swept area, rotor diameter and weight, which are 1.07 m^2(11.5 ft^2), 1.17 m (46 in) and 5.9 kg (13 lb) respectively. The alternator is a permanent magnet brushless type in all mentioned versions and another common thing among them is survival wind speed which is equal to 42 m/s.
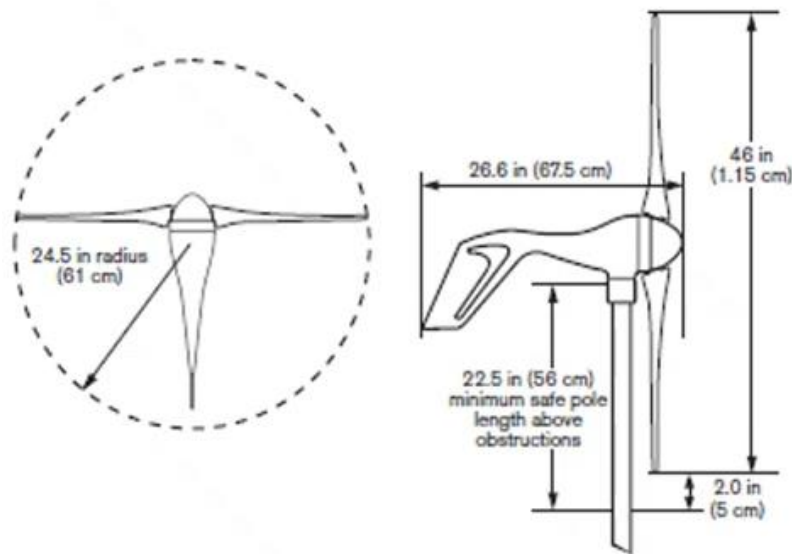
Figure 3-2 main diameters of a small wind turbine

Air Silent X is ideal for low noise applications, as it produces less than 40 decibels of sound. Moreover, the blades made of 3 injection molded composite are cheaper than the ones made of 3 hand laminated carbon fiber (which also have low sound emissions). High strength materials are used in all blades in order to resist fracturing.

Except for Air Max and Air Silent X, which have a corrosion resistant cast aluminum body, the turbines are made of permanent mold cast aluminum. One of the main advantages is shipping dimensions 686 x 318 x 229 mm (27 x 12.5 x 9 in) and weight equal to 7.7 kg (17 lb), that can be packaged in a small box making the transportation of the devices more

practical and inexpensive. cut_{in} speed varies between 3.1 and 3.58 m/s (7-8 mph) which depends on the elevation, at sea level would be lower and at elevation of 1000 feet would be higher because of air density.

Air 40/Breeze wind turbines have 30% larger surface area than Air 30/X marine wind turbine and start up at lower wind speeds, which enables them to operate in lower wind speeds and produce less noise so this type can be applicable in short towers and in consequence turbulence is much higher hence we need more surface on the blade set, but Air 30/X marine generates more energy in higher wind speed regions, which is shown in Figure 3-3.
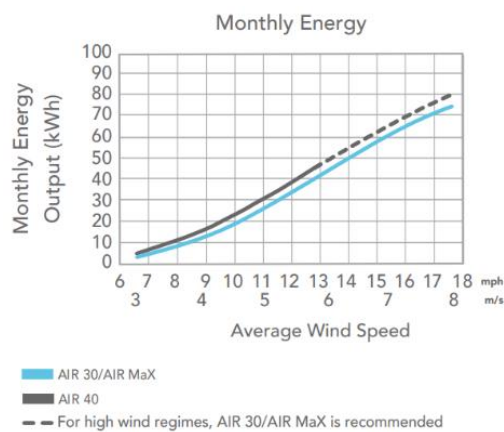
Figure 3-3 comparison of monthly energy between Air30/MAX and air 40 turbines

In Figure 3-4 the power output versus the wind speed is illustrated, in which the cut-in speed of the three main categories of wind turbines can be discovered. Additionally, the peak of power output for Air 40 turbines in higher wind speeds are much higher than the

equivalent value for air 30 and MAX turbines.

Instantaneous Power*
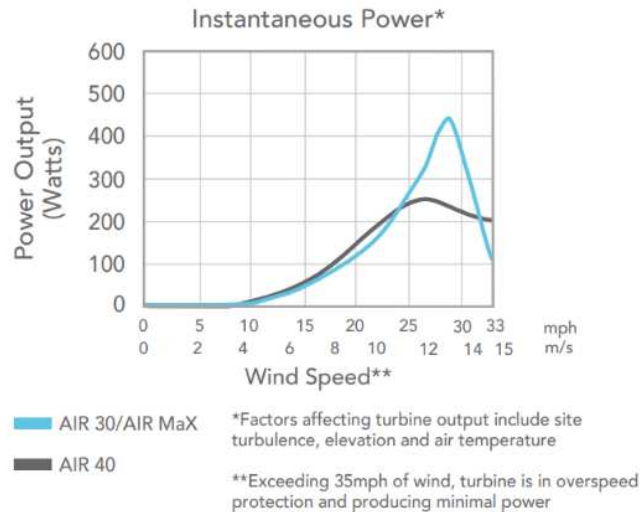
Figure 3-4 comparison of power output between air 30/ MAX and air 40 turbines

Each wind turbine operates within a certain voltage range, which is determined by the factory set point. The turbine will automatically stop when the voltage exceeds the set point by about 15 percent, and will start operating when the voltage falls below the set point by about 5 percent. The turbines with 12 volts set points stop at 14.1 volts, the ones with 24 volts set points stop at 28.2 volts, and the ones with 48 volts set points stop at 56.4 volts. The LED on the wind turbine indicates whether the turbine is on or off by blinking or being solid. The schematic of a small wind turbine is shown in Figure 3-5.

Figure 3-5 schematic of a small wind turbine

In Figure 3-6 the main components of a small wind turbine are shown. Ryse Energy [17] is also one of the leading manufactures in small and micro wind turbines which publishes

the data of power output of different kind of turbines in different wind speeds.

Figure 3-6 Components of a small wind turbine [17]

In Figure 3-7 the exploded view of the components of a small upwind horizontal axis wind turbine is shown. The tail of the turbine referred to as number 22 is designed to keep the turbine on the wind. It is installed on the yaw labeled as number 26 by slippery assemblies and bearings, which can rotate 360 degrees. This rotation enables the turbine continously track and face the wind direction. As a result of this feature, this type of turbine is referred to as a three-blade passive yaw upwind horizontal axis wind turbine.
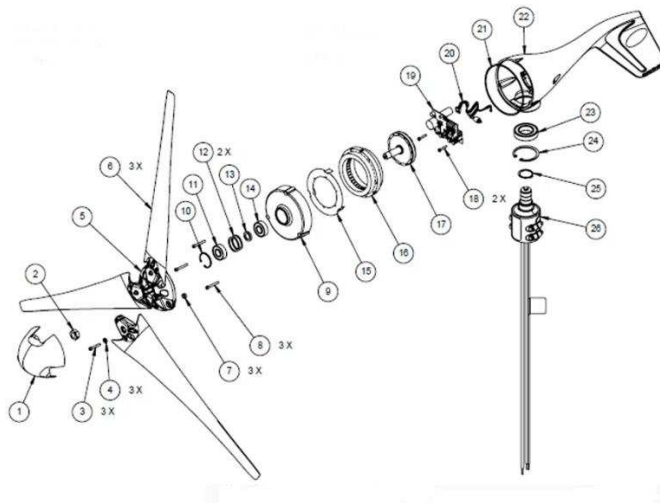
Figure 3-7 components of a small wind turbine - exploded view [16]

The importance of the nose cone and the hub in a wind turbine cannot be overstated. These components serve to cover a small gap between the rotor shaft referred to as number

9 and the bearings. By removing the nose cone, the hub, or both - for instance, when preparing for a severe weather event like a hurricane – and not replacing them after removing your blade set, water can infiltrate through the tiny gap between the rotor shaft and the bearings. The stator (number 16) of a wind turbine is equipped with neodymium magnets that encompass the rotor. This spinning action generates an electrical charge. This AC charge, is then sent through a circuit and rectified into DC voltage - either 12, 24, or 48 volts. The rectifier, referred to as number 19, is specifically matched to the voltage inside the turbine and the stator, making each of our turbines voltage-specific. Therefore, when ordering a turbine, it's essential to choose the correct voltage to match your battery bank. For instance, a 24-volt battery bank requires a 24-volt turbine. It has been suggested that the generators equipped with permanent magnets are more suitable for small-size wind turbines because of their higher efficiency compared with other generators [18].

Number 20 is the LED light. If the LED is not illuminated, it means there in no wind. If the light is illuminating slowly, it means the trubine is in regulation, in other words, the turbine reached the factory set point – for instance 14.1 voltage for 12 voltage turbines and then is shutting down by electromagneticall break. Blinking fast of the light means the high speeds of the wind turbine that also needs to shut down, this is called overspeed protection. Another important signal that can be discovered from the LED is the first two blinks which occurs after connecting to the battery bank, in other words, if there is no blinks immediately after connection, it's the sign of the wire issues.

The maintenace of wind turbine consists of inspecting the blades annually for damage, after 1-3 months after first installations and every 12 to 18 months thereafter. Tigheting yaw, blade and rotor bolts to 4, 7 and 50 lb.ft respectivel and also cycling the power to confirm the correct functionality of the LED. Average life of brushed and bearings are about 8 to 10 years.

In Figure 3-8 the digital device which is used to turn on or off the wind tubine is shown. This digital panel also provides the user the instant power, voltage, current and energy produced by the wind turbine.

Figure 3-8 digital wind turbine control panel

In Table 3-1 the technical characteristics of different type of small wind turbines such as energy produced monthly based on the average annually wind speed, cut-in speed which is the minimum wind speed required for turbine to start rotating, voltage, noise and the type of the blades are shown. In order to have lesser amount of noise, especially in residential area, the blades are made by carbon-fiber.

Table 3-1 Technical specifications of different types of small wind turbines [16]

	Energy	Start-up wind speed [m/s]	Voltage [VDC]	Sound	Blades
Air 30	30 kWh/month at 5.8 m/s	3.58	12, 24, 48	High	Black blades
Air X marine	30 kWh/month at 5.8 m/s	3.58	12, 24	High	Black blades
Air Max	90 amp - hr. per day at 5.5 m/x	3.13	12	Very low	Carbon-Fiber blades
Air silent X	90 amp - hr. per day at 5.5 m/x	3.13	12	Very low	Carbon-Fiber blades

| Air 40 | 40 kWh/month at 5.8 m/s | 3.1 | 12, 24, 48 | Low | Black blades |
| Air breeze | 40 kWh/month at 5.8 m/s | 3.1 | 12, 24, 48 | Low | Black blades |

In Table 3-2 the different small wind turbines based on their applicability is classified.

Table 3-2 Application of different small wind turbines

	Location	Application	Wind speed operating range [m/s]	Optimum speed range [m/s]
Air 30	Land	Industrial - O&G - telecom	3.6 - 22	11 - 15
Air X marine	Marine	industrial and off-shore	3.6 - 22	11 – 15
Air 40	Land	Residential and educational	3.1 - 22	4.5 - 22
Air breeze	Marine	sailing and residential	3.1 - 22	4.5 - 22

Figure 3-9 Different applications of small wind turbines

3.2. Generators (DC, PMG, IG)

In the past, most early small turbines used DC generators, including Burne's and the famous Jacoub machines in the USA. The advantages are that they can be easily controlled by the current field and are small and cheap, but on the other hand they are less efficient and have brushes and a commutator that wear out quickly. Three-phase AC permanent magnet generators (PMGs) are therefore preferred for modern systems. This shift over the last two decades is due to advances in power electronics and availability of more AC than DC products.

Nearly all modern generators are three-phase which improves the ratio of power to weight and provides a more consistent shaft torque compared to fewer phases. Even for grid connected small turbines, the typical approach is to rectify the varying frequency and voltage generator power and then invert it to produce AC power of constant voltage and frequency. In addition to being simple, PMGs with many poles (16 poles) are more efficient in low constant rpm and thus there is no need to gearbox. The maximum efficiency occurs normally at the highest voltage of the generator as for the same output power, the current is less and results in decreasing the loss of conduction and "copper".[19]

This conversion is also combined with maximum power point tracking (MPPT) is becoming standard on turbines above the micro category. Many micro-turbine charge batteries and use a much simpler control system.
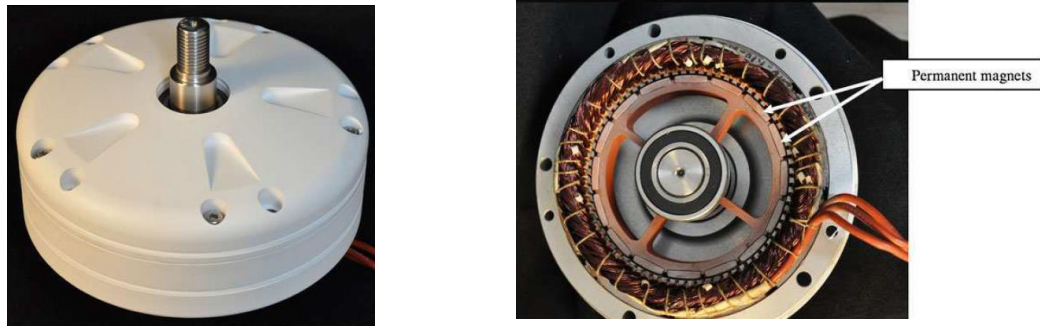
Figure 3-10 Outside and inside views of the Ginlong 500-A PMG [19]

Another more recent innovation is to combine the controller and inverter for grid connection. Filtering is commonly employed to reduce the harmonic distortion of the power supplied to the grid. The inverter must also control the power factor, and oversee the safe shutdown of the turbine if the grid is "lost". In addition, the turbine output must be synchronized with the grid.

It is also becoming common for the turbine controller to have a major or exclusive role in over-speed protection. For example, the Skystream 2.4 kW turbine, uses shorting of the PMG output instead of aerodynamic controls such as furling and pitching. As with all forms of over-speed protection, there are potential problems with shorting the output. The current or heat generated may demagnetize the magnet and/or burn out the windings.

Figure 3-11 illustrates the topology of a rectifier/controller-inverter system connected to the grid. The three-phase produced power of varying voltage and frequency so it helps the system to better matching the load because the wind turbine must operate efficiently over a wide range of loads and frequencies. If the wind turbine is charging battery, the inverter would be replaced.
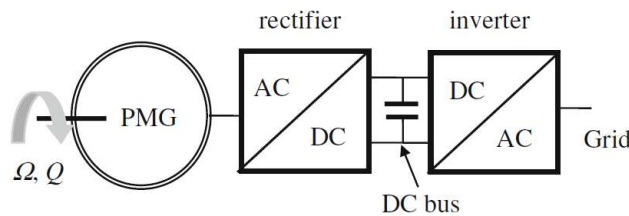
Figure 3-11 Schematic of a PMG wind turbine feeding the grid

Some small wind turbines use asynchronous or induction generators (IGs), they are usually standard induction motors running backwards. Low costs, no cogging torque and ruggedness can be considered as their main advantages. The current versions of IGs which are available in market have fewer poles compared to PMGs, they rotate more quickly and usually a gearbox is required in small wind turbine applications. The larger the wind turbine size leads to the lower frequency of the blade, thus it is also possible to design a direct drive wind turbine with an induction generator of say 8–12 poles with a rated power of between 1 and 2 kW.

3.3.   Control systems

The need for over-speed control is related to the near cubic dependence of power on wind speed, in other words, even a slightly higher wind speed rather than rated speed can cause unsafe levels of blade stress and generator power.

The main target of the control systems is to provide extensive protection for the system and condition monitoring to extend its lifetime, which can be employed using micro-processor-based controllers. For instance, the battery can be protected from being drawn too low or boot-charged. However, this control should be intelligent enough not to shut down if smoke is detected nearby barbecue.

Protection against most short-term severe damages, requires the ability to:

1. Disconnect the generator from the rest of the system.
2. Apply and disconnect any dump load.
3. Disconnect the wind turbine from any battery.
4. Disconnect the inverter from the wind turbine.

In all of these cases, an appropriate circuit braker is necessary. In Figure 3-12 the switches are shown which are installed immediately after the generator that can be used to delay the power extraction until the blades have reached the suitable rpm after starting.
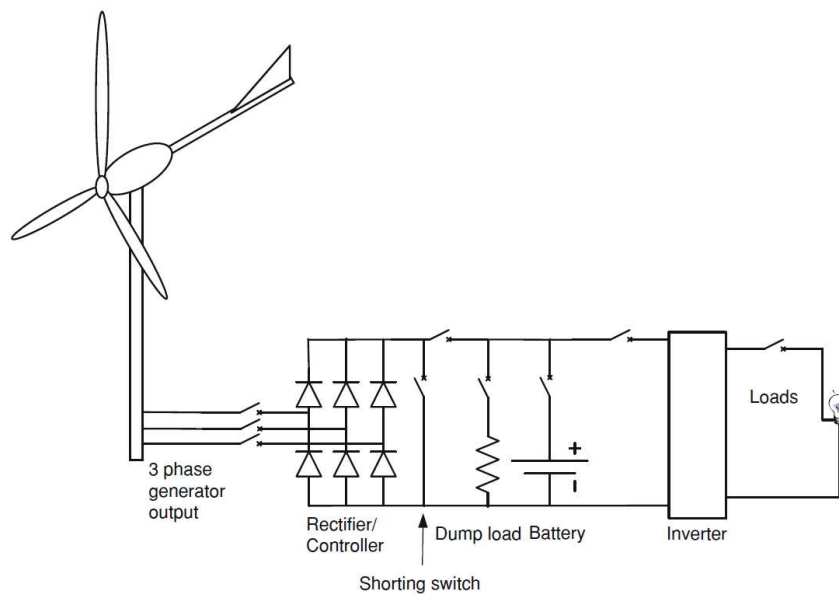
Figure 3-12 small wind turbine with basic circuit breaker and switch protection [19]

Excessive electrical current needs to be prevented by basic control protection. For example, high current causes heating and melting wires or excessive battery charging

currents results in gassing and explosion. Table 3-3 shows the possible issues and appropriate responses to control the system.

Table 3-3 Possible protection issues and responses [19]

Wind turbine		Generator		Battery (if any)		Inverter or load	
issues	response	issues	response	issues	response	issues	response
Over-speeding	Slow down Or stop	Over-current	Reduce current or disconnect	Over-charging	Stop charging	Short circuit	disconnect
Extreme winds	Shut down or stop	Over-voltage	Reduce voltage or disconnect	Excessive voltage	Stop charging	Over voltage	Disconnect
Excessive vibration	Reduce turbine speed or stop	Too hot	Reduce current or disconnect	Too low voltage	Disconnect load	Under voltage	Disconnect
Excessive noise	Reduce turbine speed	Smoke	disconnect	Too hot	Reducing load current or load current	Too hot	disconnect

When protecting against over-currents, fuses and circuit breakers are commonly used, however, it is also possible to use controlled power electronics or sacrificial components such as metal oxide varisters (MOVs). Relative reliability, simplicity are the main reason to use fuses and circuit breakers. Additionally, due to the ability to reset and easier turning off of circuit breakers are preferable over fuses.

As the majority of owners of small wind turbines rely on the produced energy even in the times of failures. In other words, even if the controller fails and leaves unprotected in strong winds), there should be a way of rescuing the wind turbine without considerable damage. Rectifiers play an essential role in small wind turbines. However, if one phase of the rectifier is damaged, it's feasible to isolate the affected phase. Depending on the damage type, the turbine can continue operating with only two phases. This may lead to increased vibration, and partial furling might be necessary to limit speed due to reduced load.

A wind turbine captures wind power and converts it into useful work. The power extracted by the wind turbine is often expressed as:

$$P = 0.5 \, \rho A C_p V^3 \tag{3.1}$$

Where power extracted from wind is defined as P, ρ the air density, the rotor area is A, the power coefficient Cp is dependent on tip speed ratio (TSR) λ and pitch angle β. V is the wind speed, λ is expressed as a relationship between V and linear velocity on the tip blade

given as:

$$\lambda = \frac{\omega R}{V} \tag{3.2}$$

ω is rotor speed and R is the rotor radius.

The optimal tip speed ratio, where the maximum efficiency is found, is provided by the equation (3.3), where n is the number of blades.[20]

$$\lambda \cong \frac{4\pi}{n} \tag{3.3}$$

Additionally, power coefficient of the wind turbine can be calculated by equation (3.4).

$$C_P = \frac{\tau.\omega}{\frac{1}{2}\rho\pi R^2 U_\infty^3} \tag{3.4}$$

Where τ is shaft torque (N.m), ω is angular speed of the turbine (rad/s) and U_∞^3 stands for free stream speed (m/s).

Considering the equation below, the denser the wind, the higher the wind speed, and the larger the rotor area, the more power that is captured. In particular, wind energy control system when connected to power grids, it should be designed to lower energy costs, at the same time ensure safe operation, comply with acoustic and power quality standards. The goal is to balance various interconnected objectives that sometimes conflict.

3.3.1. Objectives of control system

These objectives can be arranged into the following areas:

3.3.1.1. Energy Capture

Wind turbines aim to maximize energy capture within operational limits, defined by minimum (Cut_{in}) and maximum (Cut_{out}) wind speeds. Below Cut_{in}, energy gain doesn't offset operational costs, and above Cut_{out}, turbines shut down to prevent damage. Generation capacity, often depicted as a power versus wind speed curve, Figure 3-13 represents the power extracted considering physical and economic limits. In low winds (region I), the goal is maximizing energy capture; in high winds (region III), it's limiting power to avoid overloading; region II represents the transition.
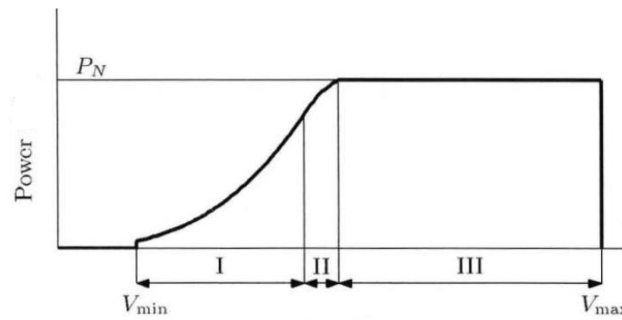
Figure 3-13 Power versus wind velocity

3.3.1.2.   Mechanical load

Main goal is not only the minimization of the cost without paying attention to other control objectives. Mechanical load, which can lead to fatigue damage and reduce the useful lifetime of the system, therefore increasing the cost of produced energy. There are two types of mechanical loads, namely static and dynamic ones. Static loads results from the interaction of the turbine with the mean wind speed. Dynamic loads are induced by the spatial and temporal distribution of the wind speed field over the swept area by the rotor and also transient loads which are induced by turbulence and gusts.

3.3.1.3.   Power quality

Power quality affects the cost of energy in several ways. For instance, poor power quality may demand additional investments in power lines, or may impose limits to the power supplied to the grid. Because of the long-term and short-term variability of the energy resource and the interaction with the power network, wind generation facilities are conventionally considered as poor-quality suppliers. Therefore, the control system design must also take power conditioning into account. This control requirement is more and more relevant as the power scale of wind generation facilities approaches the output rating of conventional power plants. Power quality is mainly assessed by the stability of frequency and voltage at the point of connection to the grid and by the emission of flicker.

3.4.   Aerodynamic control Strategies

A control system reaches its steady-state operating point when the net torque applied to the system is zero, i.e., when the generator reaction torque equals the aerodynamic torque developed on the rotor (both torques referred to the same side of the gearbox). The operating point of the wind turbine is determined by the intersection of the aerodynamic torque curve of the rotor, which depends on the wind speed and the pitch angle, and the reaction torque curve of the generator. The term control strategies denote the various ways wind turbines can be programmed to work and in particular to follow the maximum power point tracking.

In some way, the control strategy describes how the turbine is programmed to approach in steady-

state the ideal power curve in the power - wind speed plane in Figure 3-13.

Figure 3-14 illustrates the different types of power controls in the operational range of wind speeds.
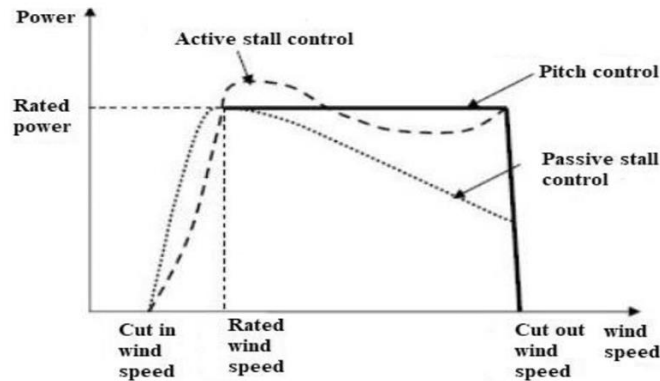

Figure 3-14 Power controls of Wind turbines[21]

3.4.1. Fixed speed – fixed pitch

In this scheme, the asynchronous electric machine is directly coupled to the power network. Thus, its torque characteristic cannot be modified which means changing pitch angle and rotational speed is impractical. Consequently, the generator speed is locked to the power line frequency Since no extra hardware is purposely added to implement the control strategy, FS-FP are very simple and low-cost. As an adverse consequence, their performance is rather poor. In fact, no active control action can be done to alleviate mechanical loads and improve power quality.

The angle of attack increases as the wind speed rises the airflow detaches from the airfoil's upper surface when the angle of attack surpasses a certain limit. This method is called stall regulation at high wind speeds. This reduces the lift and increases abruptly the drag, leads to a large increment of the axial thrust force whereas the tangential force decreases slightly. As a result, the aerodynamic torque and power decrease.

Figure 3-15 illustrates the ideal and real power curve and conversion efficiency versus wind speed values for fixed-speed, fixed-pitch control system. The point F corresponds Cut_{in} wind speed (V_{min}) whereas point D determines the maximum power that can be extracted where the reaction torque characteristic intersects the stall front. Higher wind speed leads to Passing through stall and in consequence to lower aerodynamic power. This is why operating point moves back along the generator torque characteristic until point G related to the Cut_{out}. It can also be observed the ideal power curve differs from the real extracted power. This implies reduced energy capture. The turbine achieves maximum efficiency only at one point (point E) in the low wind speed region. In higher wind speeds, the power control is not effective.
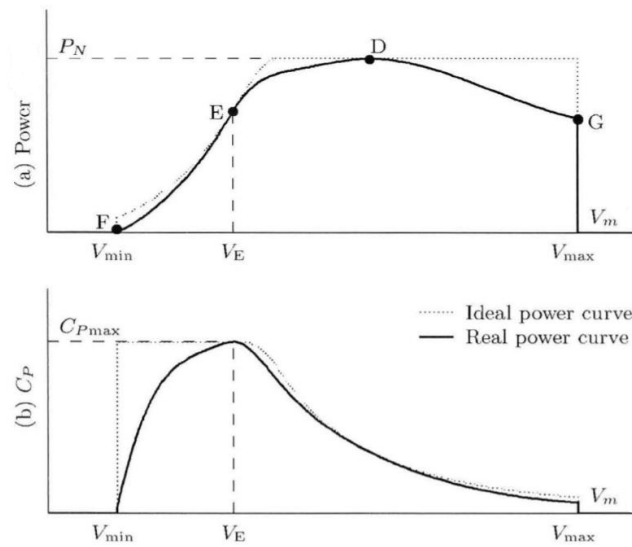
Figure 3-15 (a) output power vs wind speed, (b) conversion efficiency vs wind speed

3.4.2. Fixed speed – variable pitch

Active pitch control achieves power limitation above rated wind speed by rotating all or part of each blade about its axis in the direction by reducing the angle of attack towards father or increasing it towards stall condition. This method divides into two main categories: pitch-to-feather and pitch-to-stall.

- **Pitch to feather**

This method essentially consists in feathering the blades as wind speed rises. Thus, it is based on an aerodynamic phenomenon completely different to stall. When the wind speed increases the angle that the relative airflow makes with the rotor rises, as response the controller increases the pitch angle in order to decrease the angle of attack. Consequently, the lift coefficient C_L drops whereas the drag coefficient C_D remains constantly low. Contrary to what happens with passive stall. The thrust force f_r decreases as wind speed rises. The main advantage of this method is decreasing the thrust force which is responsible for aerodynamic loading on the structure. As a disadvantage, this method requires a considerable control effort to change the pitch angle from $0°$ to $30°$.

- **Pitch to stall**

in this method, the pitch angle is adjusted in the opposite direction of the approach above. In fact, as wind speed rises, the pitch angle is reduced in order to increase the angle of attack and due to the better control flexibility, this method's features are better than passive stall method where the pitch angle can't be modified. As a main advantage, the required control effort is low, achieving the objectives of power limitation by changing the pitch angle from $0°$ to $-5°$ is practical which is much lower compared to the active pitch control. the drawback of this method, as well as all methods based on stall, is that the thrust force increases. This type of active stall control achieves power limitation above rated power by

pitching the blades to stall in the opposite direction to that employed for active pitch control. This is why in some references is also known as negative pitch control.

In Figure 3-16 the real and ideal curves of extracted power and conversion efficiency is plotted. Since there is no control on the reaction torque, rotational speed is almost constant all along the operating locus. Below rated wind speed, the control strategy is similar to the fixed-speed fixed pitch and above rated wind speed, the controller adjusts the pitch angle to regulate aerodynamic power at rated power with the characteristic of point D.
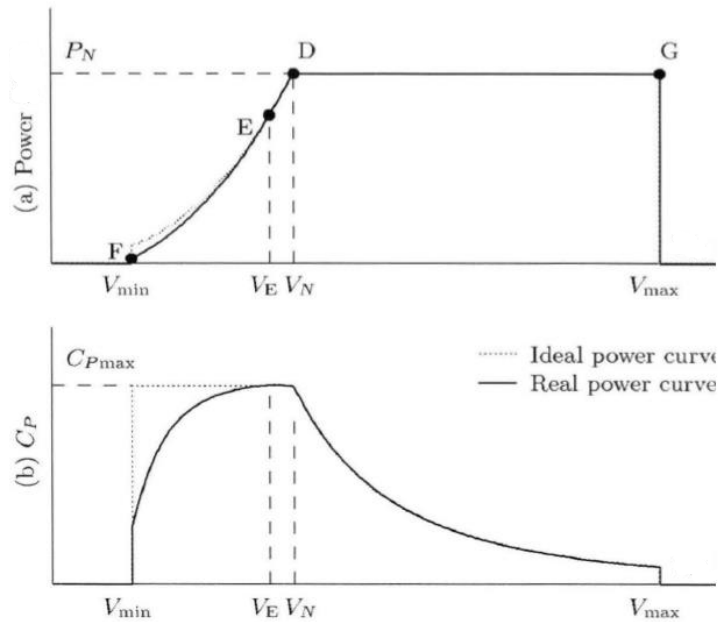

Figure 3-16 (a) output power vs wind speed, (b) conversion efficiency vs wind speed

3.4.3. Variable speed – fixed pitch

Commercial wind turbines utilize more and more variable-speed fixed-pitch, especially for low wind speed operation. Variable-speed operation offers advantages such as increased energy capture, reduced dynamic loads and improved power quality. Below rated power in order to maximize the conversion efficiency pitch angle and tip-speed-ratio must be kept constant. In low wind speeds, variable-speed wind turbines are controlled to track more or less tightly this $C_{p,max}$ locus, Based on Equation (3.5) the rotor speed must be changed proportionally to the wind speed.

$$\omega = \frac{\lambda V}{R} \tag{3.5}$$

there are basically two approaches based on passive and speed-assisted stall:

- **Variable Speed with Passive Stall Regulation**

In this scheme wind turbine operates at two modes through its whole operation region. Below rated power the main goal is to track the maximum conversion efficiency by changing rotational speed proportionally to wind turbine to maintain tip-speed-ratio, so this

part is known as variable speed and above rated power the performance is like fixed speed and fixed pitch control system with limiting power by passive stall.

In Figure 3-17 it is obvious the real power curve is attached to the ideal one in wind speeds below rated power. Note that the generator torque characteristic containing the segment ED passes through the intersection point between the rated power hyperbola and the stall front. This is to capture as much energy as possible without over loading. In the region with greater wind speed compared to rated speed, there is a superposition of operating points in segment GD.
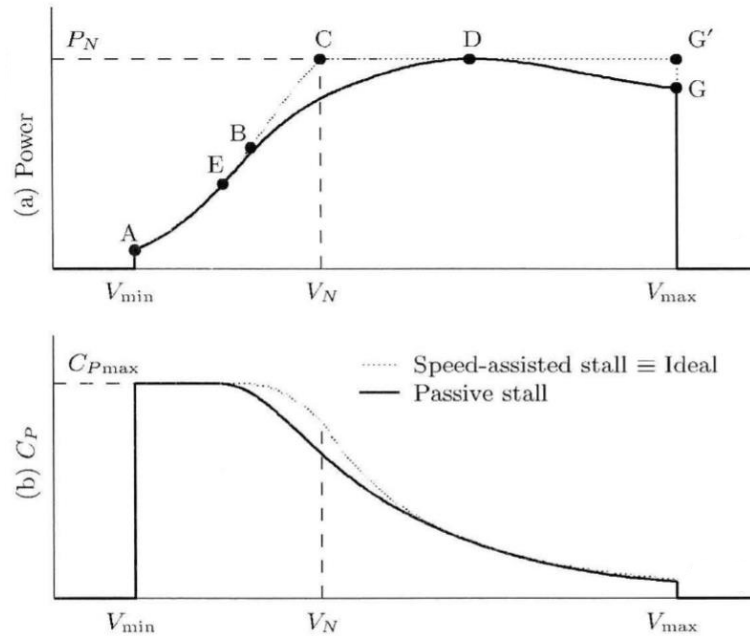

Figure 3-17 (a) output power vs wind speed, (b) conversion efficiency vs wind speed

- **Variable Speed with Assisted Stall Regulation**

The control strategy coincides with the $C_{P\,max}$ curve from A to B. All along this curve, rotational speed increases proportionally to wind speed until rated speed is reached at B. Since ω cannot be exceeded, the operating point moves along the segment BC. For wind speeds above rated, the operating point moves along the rated power hyperbola towards the stall front. At wind speed V_D, the control strategy reaches the stall front, i.e., the turbine stalls. For higher wind speeds the operating point moves back along the hyperbola until shut-clown at G'. Although this control strategy potentially enables maximum energy capture, it also brings with it some transient problems.

3.4.4. Variable speed – variable pitch

Variable-speed variable-pitch control strategies are being more and more common in commercial wind turbines. In this scheme, the turbine is programmed to operate at variable speed and fixed pitch below rated wind speed and at variable pitch above rated wind speed. Both pitch-to-feather and pitch-to-stall strategies can be followed. In low wind speeds, the turbine is operated along the $C_{P\,max}$ curve between the points A and B. At point B, the

rotational speed gets to its upper limit ω_N. Therefore, rotational speed is regulated at this value on the segment BC as wind speed increases from $V_{\omega N}$ to V_N. Variable-speed operation increases the energy capture at low wind speeds whereas variable-pitch operation enables an efficient power regulation at higher than rated wind speeds. In addition, variable-pitch operation alleviates transient loads. This is an important advantage of this control strategy in comparison with VS-FP ones, particularly for large-scale wind turbines.

3.4.5. Yaw control

As shown in Figure 3-7, the tail assembly and bearings enable the wind turbine system to track the wind direction. This allows the turbine to face the wind and extract a greater amount of energy.

However, there are two factors that prevent the system from responding quickly to limit power. The first is the significant moment of inertia of the nacelle and rotor about the yaw axis. The second is the cosine relationship between the component of wind speed normal to the rotor disc and the yaw angle. This relationship means that for small initial yaw angles, changes in yaw of, say, 10° will result in only a small reduction in power output - just a few percent. In contrast, blade pitch changes of the same magnitude can easily reduce the power output by half.

3.5.   Effect of turbulence of the wind on the wind turbine

Turbulence, a characteristic of wind flow, significantly affects wind turbine performance by changing the wind speed profile and exerting considerable stress on the blades. This inflow has significant impact on the loads and ultimately its lifespan. Turbulent statistics can be extracted from simulations such as mesoscale and fine-scale, numerical weather prediction models and large eddy simulations (LES). while LES models require substantial computational resources to simulate long periods of time, mesoscale models offer a more efficient alternative and also is able to estimate the turbulent kinetic energy (TKE).[22]

Turbulence intensity (TI) is defined as the standard deviation of the horizontal wind speed (σ_U) divided by the average horizontal wind speed ($\bar{U}$) over a time interval, are shown in equation (3.6) and, (3.7) respectively.

$$TI = \frac{\sigma_U}{\bar{U}} \tag{3.6}$$

$$\bar{U} = \sqrt{u^2 + v^2} \tag{3.7}$$

Horizontal wind vectors (u and v) from the reference lidar were calculated at ~1 Hz using the raw radial velocity measurements along the cardinal directions.

The turbulent kinetic energy is defined as:

$$TKE = \sigma_U^2 + \sigma_v^2 + \sigma_w^2 \tag{3.8}$$

where σ_U^2, σ_v^2 and σ_w^2 are the variances of zonal, meridional, and vertical wind components, respectively.

Measurements of turbulence are often made by using instruments located within the flow or in situ, such as with cup, propeller or sonic anemometers. Power production can fluctuate by up to 20% at wind speeds of approximately 8 m/s, depending on turbulence intensity.[23]

According to the Ishihara model, the turbulence's impact is strongly related to the ground conditions and any obstacle, significantly affecting a wind turbine's power output. Generally, it has been found that a rise in the ambient turbulence level on an energy-producing turbine consistently leads to an enhancement in the turbine's mechanical power and an increase in the blade loads. The impact of turbulence on turbine power output is assessed, using calculations for various speeds (6-9 m/s) on the active disk, For a roughness of 0.3 m of agricultural land with many hedgerows, both with and without turbulence. The results summarized in Table 3-4, reveal that turbulence increases power output, especially in turbines further from the turbulent flow source. The maximum difference occurs at a dimensionless distance of x/D = 8.[24]

Table 3-4 Effect of turbulence on the power of the wind turbine [24]

U [m/s]	Maximum difference Δp (kW)
6	10.22
7	18.70
8	29.03
9	41.28

S. Lee and M. Churchfield employed large-eddy simulations to investigate the influence of four different atmospheric conditions and surface roughness on the structural loadings of wind turbines (2 NREL[1] 5-MW) with the average hub-height of 8 m/s which is below rated speed. Structural load data are collected using the aeroelastic tool, FAST coupled with LES[2] solver. Histograms of stress range indicate that the surface roughness has a strong influence on the extreme loadings on the turbine, where higher roughness leads to increased damage equivalent loads (DELs). The atmospheric instability appears to have a weak impact on the DELs.[25]

Miguel Talavera et al at the Department of Aerospace and Mechanical Engineering, New

---

[1] National Renewable Energy Laboratory   [2] Large Eddy Simulation

Mexico State University in their wind tunnel by installing two wind turbines with different distances in relation to the issue of unmatched Reynolds numbers for downscaled wind turbine under laminar and turbulent inflow which was made by active grid system found out that wind power decreases under laminar flow and the reason is the flow separation around the wind turbine blades. The more the flow gets separated, the more the power drops. In laminar flow, more than 50% of the blade is covered by separating bubbles, compared to 25% in turbulent flow.[26]

Another study was carried out by A. Al-Abadi et al in an optimized laboratory scale wind turbine by torque matched aerodynamic shaped method (TMASO). The objective of this investigation was finding out the impact of turbulence on performance of wind turbine. This was done by exposing a wind turbine to different turbulent levels, created by fine and coarse static grids, as well as in the absence of grid. It has been discovered that at higher turbulence level, power coefficient and also tip speed ratio rise leading to increase the rotational speed, given that the wind speed is constant. This is due to more interaction between blade surface layer and the stream, which leads to limit the flow separation and consequently delaying the stall (loss of lift) and also due to the help in damping the tip vortices by adding winglets.[27]

The effect of different turbulence intensities on wind energy production of a small wind turbine (Bergey XL.1, 2.5-meter diameter blade with rated capacity of 1 kW installed on an 18 m tall, 0.114 m diameter galvanized steel tubular tilt-up tower) has been investigated. the turbulence intensity categories are classified based on turbulence intensity (standard deviation divided by the mean wind speed), where the median turbulence intensity for the entire dataset was 0.173. Low turbulence intensity was classified as turbulence intensity less than 0.14. Turbulence intensity greater than 0.18 was considered high. This study exhibits the cut-in speed of 4 m/s and begun furling at 9 m/s. In the range of operation, low turbulence intensity results in reduced power output (around -2%) likely due to reduction in intermittent furling and associated hunting, conversely the high turbulence intensity leads to increase the output power (approximately 0 to +4%). Turbine energy production lagged changes in wind speed by one to two seconds. [28]

At the Ashikaga University in Japan, a small 135 W wind turbine was installed close to the roof of a 5 m high building. It was found that the output power of the turbine was dependent on the wind speed. At low wind speeds, the output was higher because the rotational speed could follow the variations in wind speed, allowing the increased energy of the wind to be captured. In contrast, at higher wind speeds around the shutdown speed, higher TIs caused early shutdown due to momentary high-speed gusts.[29]

Luisa et al. installed two small commercial wind turbines, horizontal (HAWT) and vertical (VAWT) axis and characterized by the same rated power of 20 kW, in the port of Savona (northern Italy). Firstly, it has been concluded that due to the higher swept area of horizontal wind turbine, it's extracted energy is higher than vertical one. Secondly, this analysis shows that the ambient turbulence cannot be considered as the main reason for such

a high production loss, which is probably caused by other technical problems that could be related to an inadequacy to high turbulence level flows.[30]

3.6.   Challenges with small-scale wind turbines

It is clear since now the developments in wind energy capturing are mainly concentrated towards large scale power production. On one hand, the primary reason for the preference of Large-Scale wind turbines (LSWTs) is the economy of scale, which makes their installation and operational cost justifiable. On the other hand, Small-Scale wind turbines (SSWTs) are less adaptable due to two main factors: poor aerodynamic performance and low power output. The aerodynamic performance of a wind turbine is primarily determined by the Reynolds number of the airfoil used in the turbine blades.

The Reynolds number of an airfoil is given by:

$$Re = \frac{\rho c u_{rel}}{\mu} \tag{3.9}$$

where ρ and μ are the density and dynamic viscosity of air, respectively; c denotes the cord length of the airfoil; and u_{rel} is the relative wind speed. Relative wind velocity is vector sum of the wind velocity and blade velocity at mid-radius of the rotor. Mathematically it is given by:

$$u_{rel} = u_{\infty} + u \tag{3.10}$$

where u_{∞} is the upstream free wind velocity and u is the velocity of the blade, whose magnitude is equal to $r_m . \omega$. In which r_m is the mid-radius of the wind turbine rotor and ω is the angular velocity of the rotor. When a wind turbine rotor is stationary, the relative wind speed with respect to the turbine blade is constant from root to tip of the blade and it is equal to the actual wind speed.

In Table 3-5 some of the current horizontal axis small to mid-scale wind turbines are mentioned with their rotor diameter and the rated wind speed to achieve the rated power and overall efficiency.

Table 3-5 Some of the currently available small-to-mid-scale HAWTs

Sr. No.	Description	Rotor diameter (cm)	Rated wind speed (m/s)	Overall efficiency[a]
1	NE-100 S	120	10	14%
2	NE-200 S	130	11	18%
3	NE-300 S	130	13	17%
4	Energy Ball V100	110	10	17%
5	Micro Wind Turbine	23.4	2–7[b]	18%[c]
6	Bornay 600	200	11	23%
7	AC 120	120	9	24%
8	AC 240	165	9	25%
9	µF500	50	12	25%
10	Superwind 350	120	12.5	26%

Given by equation (3.9), Reynolds number is proportional to the cord length and the wind speed. These two factors have very small values, therefore small wind turbines are operating in the very small values of Reynolds number in comparison with large-scale wind turbines.

In Figure 3-18 the effect of Reynolds number on the lift and drag coefficients of a NACA 0012 airfoil is depicted.[31]
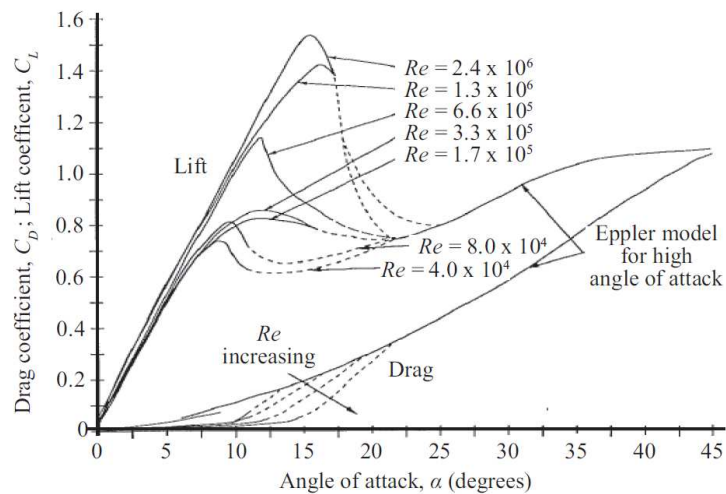
Figure 3-18 Influence of Reynolds number on airfoil behavior (NACA-0012) [31]

It is noteworthy that the maximum lift coefficient decreases when Reynolds number decreases, while drag coefficient increases. This means that the lift-to-drag ratio drops significantly with a decrease in Reynolds number, resulting in a poor aerodynamic performance of small wind turbines. Therefore, the first and foremost step in selecting a suitable airfoil is to ensure the compatibility of the Reynolds number which is crucial to achieve good performance for small-scale wind turbines.

The power P generated by a wind turbine is given by following expression:

$$P = \frac{1}{2}\eta\rho\pi r^2 u_\infty^3 \qquad\qquad (3.11)$$

where r is the radius of the wind turbine, u_∞ is the speed of wind. η denotes the overall efficiency of the system whose maximum theoretical value is 16/27 (Betz's limit) and accounts for various losses in the wind turbine, such as blade losses in the rotor, frictional losses in the bearings, and electromagnetic losses in the electric generator. The power output is proportional to the square of the radius of the wind turbine and the cube of the wind speed. As the turbine size and wind speed decrease, the output drops dramatically and below a certain limit is too small to justify the cost of construction and operation.

Another important factor that needs to be considered is the cut-in speed, known as the minimum required wind speed at which the turbine begins to generate power. Overall inertia and internal friction of the system including components like the rotor, ball, bearings, gear train and generator are the main factors influence the cut-in speed. As the size of the wind turbine decreases, the cut-in speed typically lowers due to the reduced inertia of the turbine blades. However, a smaller blade size also decreases the aerodynamic torque, which in turn increases the cut-in speed. Balancing these two contrasting factors is crucial in designing a small wind turbine with an optimal cut-in speed and power output.

It can be a challenge to achieve the desired revolutions per minute (rpm) of the generator. It's important to select a small generator with low starting torque and a high voltage-to-speed ratio. If a gearbox is necessary, the choice of gear ratio is important as it is a function of the speed and torque range required for optimum generator performance. The size of the nacelle can also be a constraint on the size of the gearbox and therefore the gear ratio. When finalizing the gearing system, cost, noise and operational reliability are important considerations.

Optimizing certain geometric parameters of the wind turbine blades, such as twist angle, blade angle, taper angle, chord length, strength and number of blades, is also essential. However, most design tools have been developed for Large-Scale Wind Turbines (LSWTs), and Small-Scale Wind Turbines (SSWTs) require different tools because of their unique aerodynamic performance. SSWTs are smaller, operate at lower wind speeds and are often located close to the ground where wind conditions are weaker and more turbulent. Therefore, the design objective for SSWTs is not only to achieve maximum power output, but also high starting torque at low wind speeds.[32]

4. Numerical Model

4.1.   Laboratory model

The chair of turbomachinery at the University of Duisburg-Essen has designated a specific room on the second floor of one of the laboratories in department MD for the study of small wind turbine technology. In order to simulate the conditions of a real-world wind environment for the study of the wind turbine, an axial compressor has been incorporated into the setup. The outlet air from the axial compressor is directed towards the wind turbine through an exhaust channel, creating a controllable airflow. This arrangement is a practical approach that make an in-depth analysis of the small wind turbine's performance under a variety of wind conditions more manageable and easier to understand, which contributes to the ongoing research in the field of wind turbine design.

Additionally in order to ensure that the noise level is kept to a minimum, two rows of silencers, which are shown in Figure 4-2, are installed in the exhaust channel of the compressor. This is particularly important given the location within the university laboratory which is shown in Figure 4-3.

Figure 4-1 represents the different parts of the axial compressor in the laboratory of the chair of turbomachinery in the university of Duisburg-Essen.
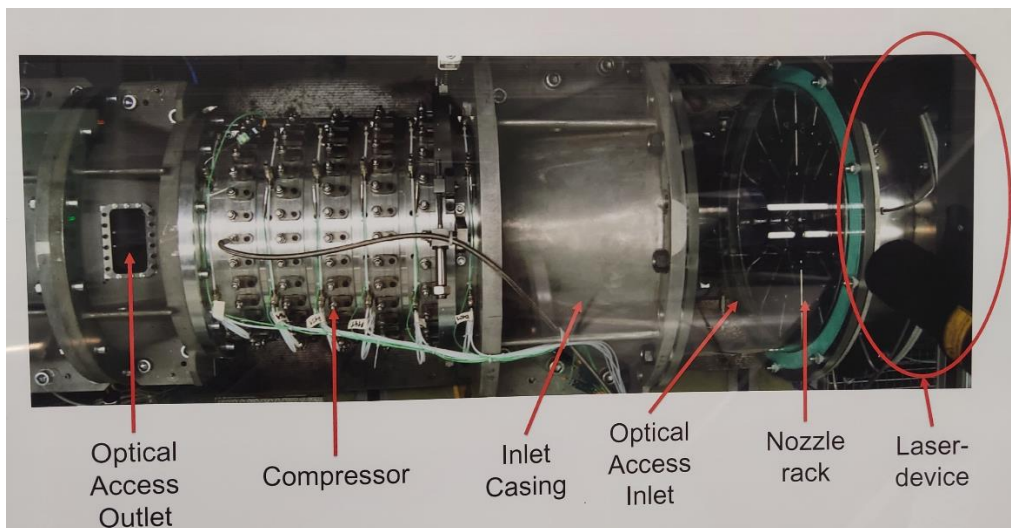
Figure 4-1 Axial compressor in the chair of turbomachinery, Duisburg Germany

Figure 4-2 Silencers

Figure 4-3 Room

In this research, Ansys ICEM is used to model the experimental configuration including the exhaust channel from the outlet of the compressor and then silencers and reaching an internal wall with a circle hole with the diameter of 1.5 meter exactly in the middle of it and finally the designated room. In Figure 4-4 the Ansys ICEM model of the exhaust channel and its inlet, two rows of silencers, internal wall and the room and the outlet is illustrated.
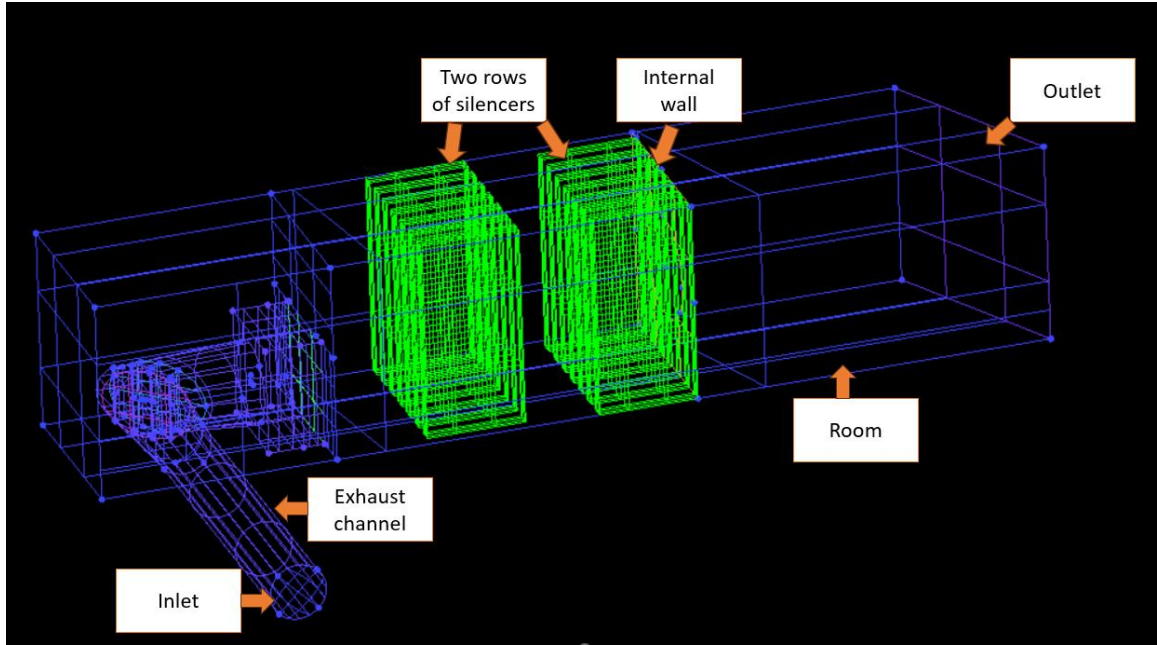
Figure 4-4 Exhaust channel, silencers, internal wall and room model in Ansys ICEM

4.1.1. Exhaust channel

The first part of the model consisting of exhaust channel has been generated using structural mesh and silencers and room has been formed with unstructured mesh. The structured mesh is employed using the blocking tool and then splitting the block and association with curves and points of the geometry. Additionally. In order to be more precise O-grid tool has been used to have a better association of the exhaust channel and therefore better mesh.
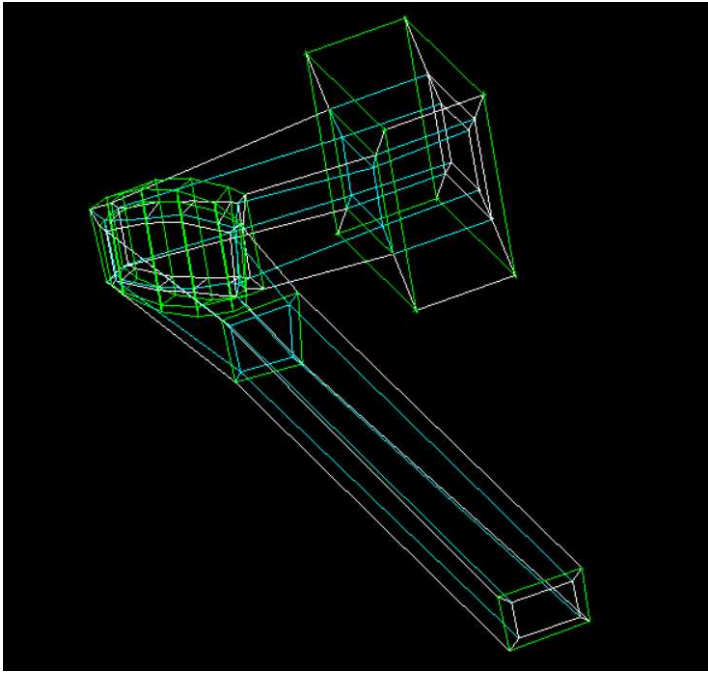
Figure 4-5 blocking of exhaust channel
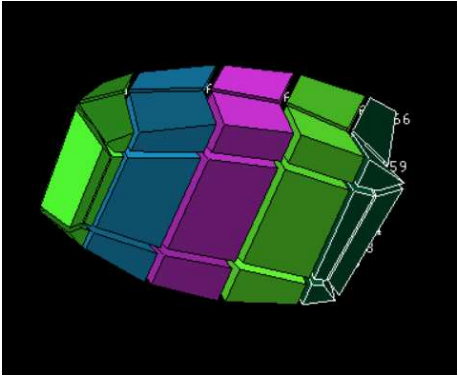
(a)
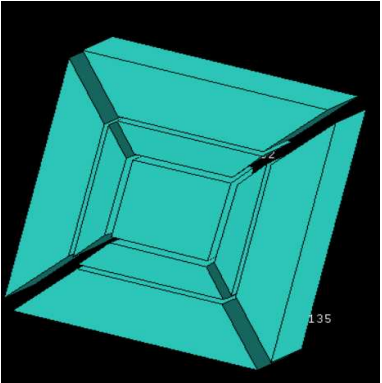
(b)
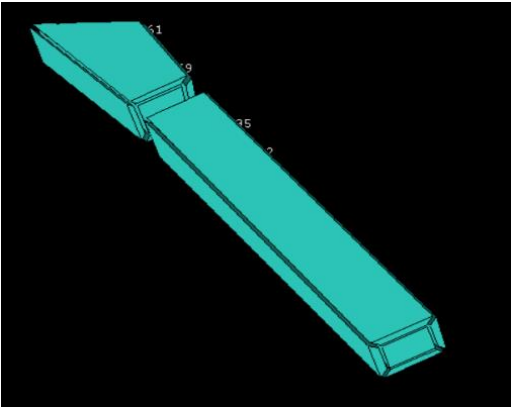
(c)

Figure 4-6 blocks of exhaust channel: (a) corner, (b) outlet, (c) Inlet

4.1.2. Silencers

Figure 4-7 illustrates surfaces of the two rows of silencers installed inside the room in order to decrease the noise of the flow in high range of flow speeds. Internal wall is installed to get the higher values of flow speeds and more homogenous flow inside the room
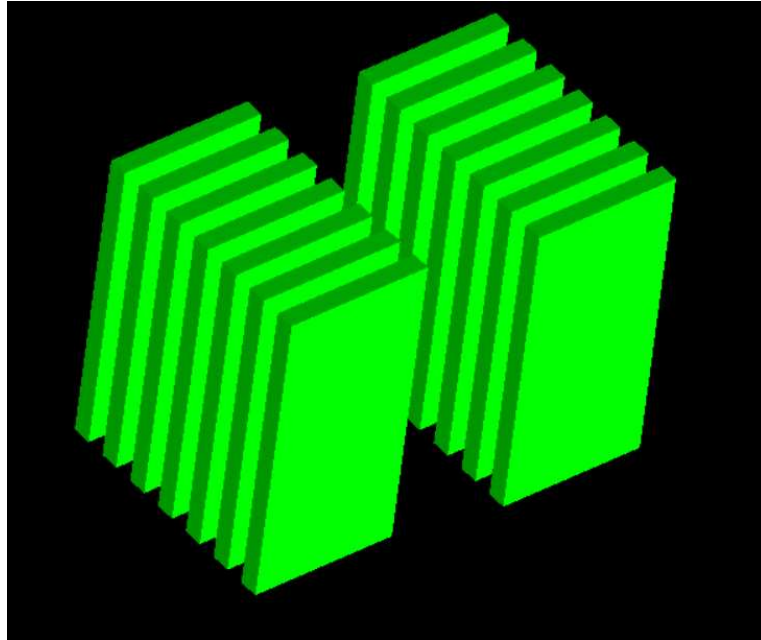
Figure 4-7 Two rows of silencers

4.1.3. Internal wall

In order to improve the homogeneity of the air flow inside the room, a wall can be installed with a centrally located hole measuring 1.5 m in diameter in the middle can be installed. As depicted in Figure 4-8 the internal wall is designed at the entrance of the room. precisely on the silencers.
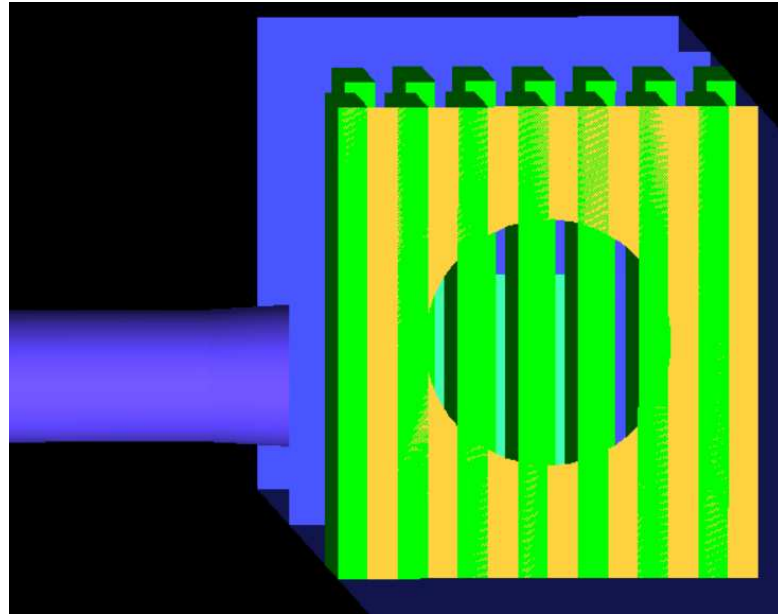
Figure 4-8 Internal Wall

4.1.4. Honey comb

One of the most useful ideas to increase the velocity and homogeneity of the flow after the silencers is to install a honeycomb. Honey comb is a 1.5-meter diameter cylinder exactly the same as the diameter of the hole inside the interna wall. The designed honey comb consists of two parts, a cylinder with 20 cm length and then 2 cm porous domain. in this research the effect of this honey comb on the velocity and homogeneity of the flow has been assessed with different values of porosities. In Figure 4-9 the honeycomb is depicted.
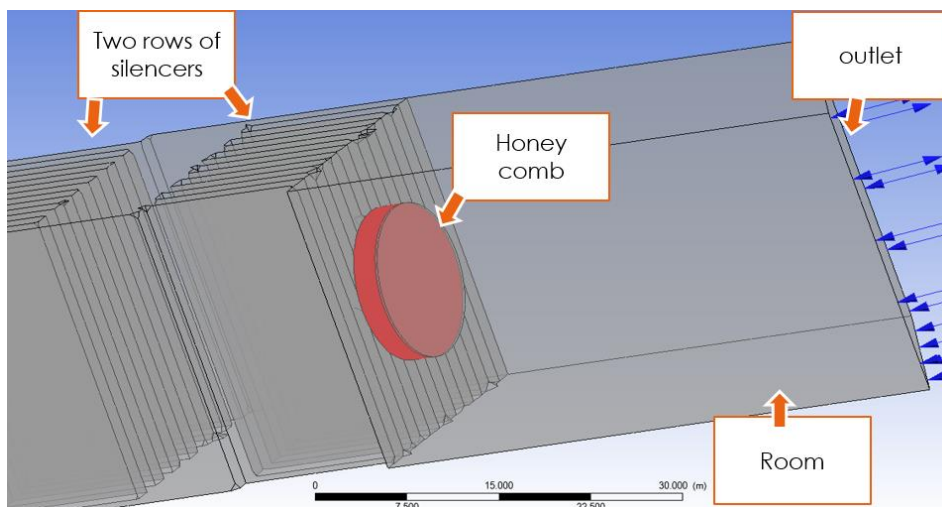
Figure 4-9 Honey comb

4.1.5. CFX Setup (Ansys)

Figure 4-10 illustrates generation of both structured and unstructured mesh for exhaust channel and room respectively in Ansys ICEM software.
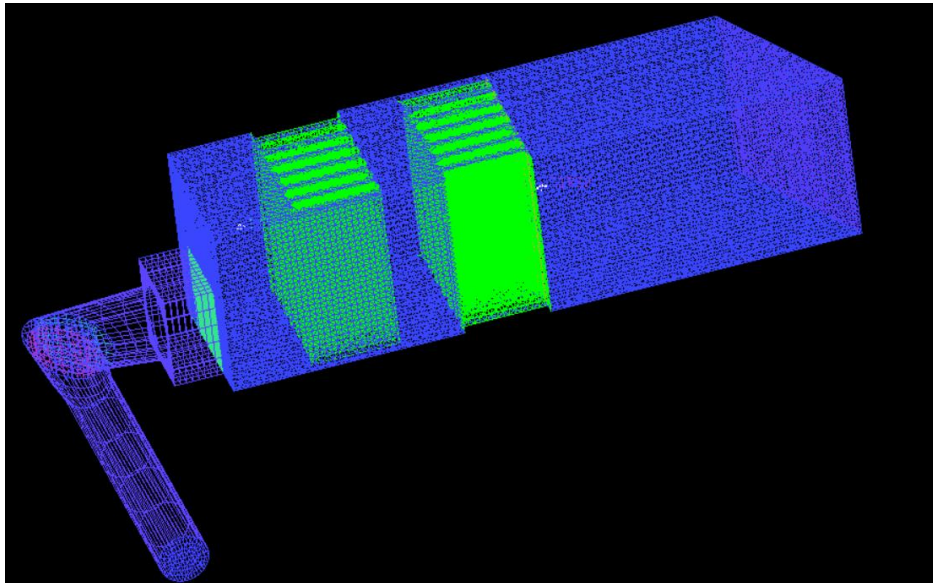
Figure 4-10 meshing the laboratory model

In Figure 4-11 the requirement of setting up the CFX for the exhaust channel and the designated room. CFX tool enables the user to define the boundary conditions in order to define the inlet, outlet, internal walls and interfaces.
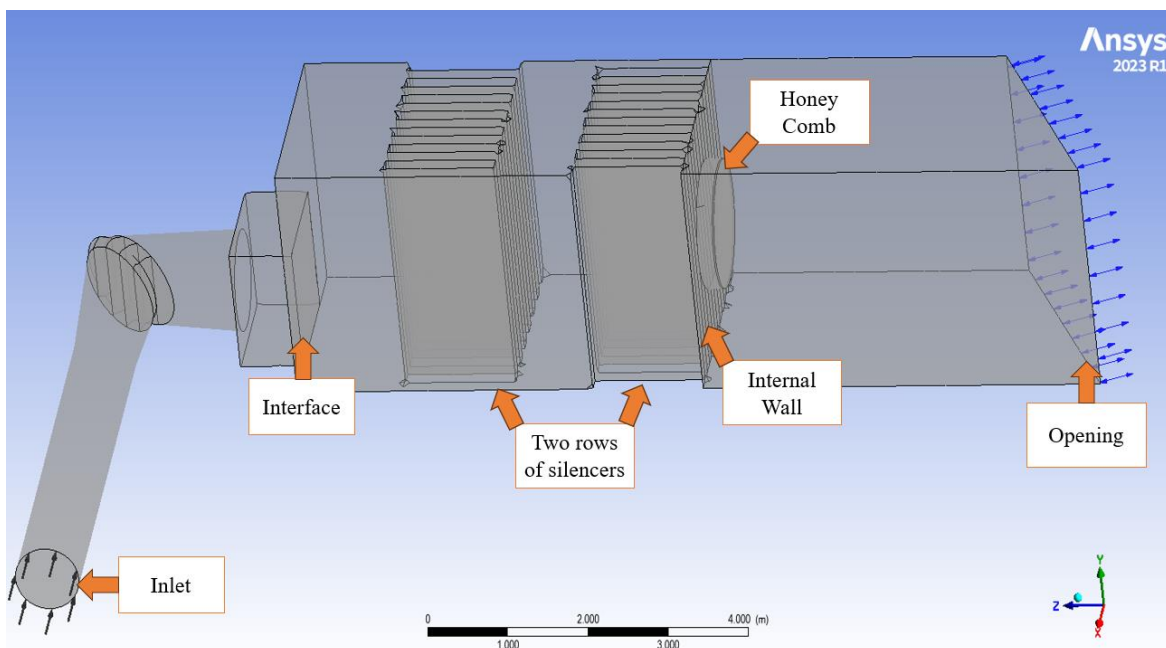

Figure 4-11 CFX Setup of the exhaust channel and the room

47

The domains and their corresponding boundary conditions have been defined. The structured mesh part has been defined in one domain with the boundary conditions of "inlet" and "Mass flow rates" equal to three different values and "total temperature" equal to 65℃. The temperature of the flow at the inlet has been defined based on the outflow of the compressor. One domain for the first part of the room and other domain consisting of the second part of the room, honeycomb and outlet of the flow.

The boundary condition of the wall has been defined for the honey comb and internal wall. The reason why "opening" has been selected for the outflow, was that by choosing "outlet" Anys assigns the outlet as a wall which is not realistic.

4.1.6. CFX Solver Manager (Ansys)

Once the domains and their corresponding boundary conditions and interfaces were ready, by defining solver control parameters as "High resolution" and maximum number of iterations equal to 10000 and using advection time scale equal to 0.105s for the "Physical timescale".

4.1.7. CFD Post-Processing (Ansys)

Post-processing in Computational Fluid Dynamics (CFD) is a critical step that involves the analysis and visualization of the results obtained from the simulations. These visualizations can include contour plots, vector plots, or streamlines that represent fluid flow patterns, pressure distributions, or temperature gradients. By studying these visualizations, we can gain valuable insights into the behavior of the fluid flow, validate our simulation against experimental or analytical results, and make informed decisions for design optimization. This step is the last step of assessing the geometry under defined conditions.

In this work, the final aim is to understand better the flow arrangement in the room in terms of velocity and deviation from the average velocity in different interactions with the wind turbine. In order to achieve this goal, circular planes with the same diameter as a hole inside an internal wall (1.5 meter) have been defined in different distances from the internal wall. The distance between each plane is equal to 20 cm, which are illustrated in Figure 4-12.
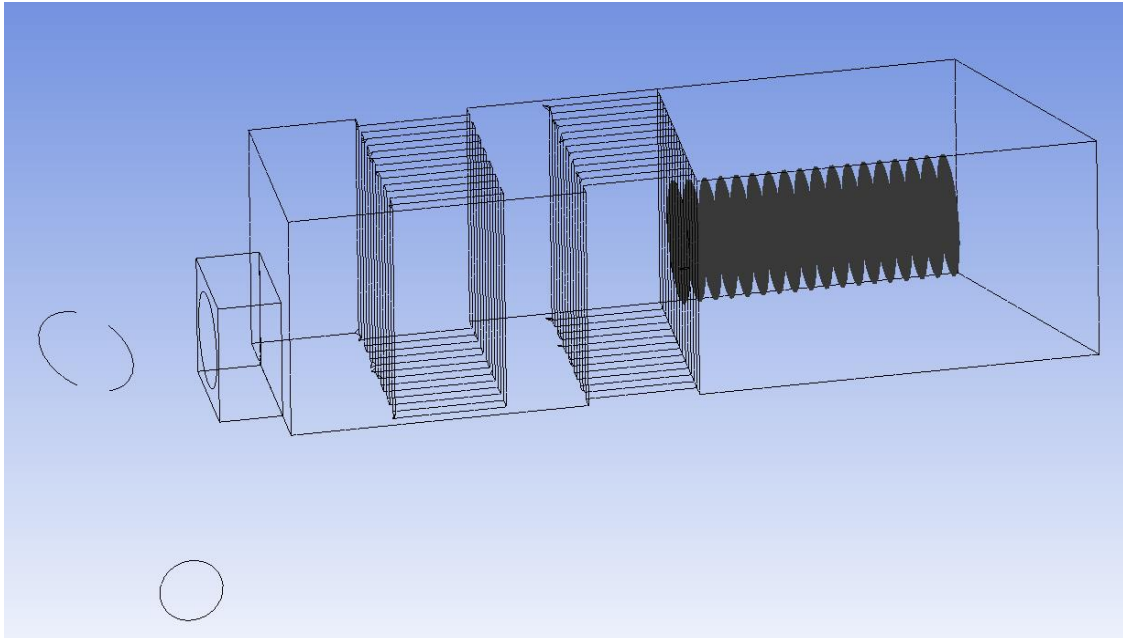
Figure 4-12 CFD-Post Processing, circular planes in the room

the best location to install the wind turbine inside the room will be determined based on the velocity values and also the homogeny of the flow in different distances from the internal wall.

In the following section, the methodology used in this work to analyze the air30 wind turbine will be well defined.

4.2. Air 30 wind turbine

4.2.1. Blade (Creo Parametric)

In the context of this research, a blade of small wind turbine from the manufacturer Primus Wind Turbine[16] was selected for evaluation. Additionally, in section 3 all of the products' characteristics of this company including the length, swept area, extracted energy, the optimum and operational range of wind speed and important specifications are described in detail. The air 30 blade has been scanned by a 3D scanner in one company in Duisburg Germany and we have been provided by the file of Creo parametric and Ansys ICEM of the blade. These files contain all of the sections connected to each other as a body, including leading edge, trailing edge and bolts section of the blade enabling it to be connected to the hub.

Figure 4-13 depicts the of the blade of the wind turbine used in this study.

Figure 4-13 Air 30 blades

In Figure 4-14 the model of the scanned blade inside the Creo parametric software is illustrated.

Figure 4-14 Creo Parametric Model

4.2.2. Hub (Creo Parametric)

A cylindrical tube with two round surfaces in the front and rear part of the blade has been modelled inside Creo Parametric software and then coupled with the blade. The main reason

of the round surfaces for the front section is to avoid flat surfaces in the direct contact with the wind coming from upstream and reduce the losses due to the sharp edges for the rear section.

In Figure 4-15 illustrates the hub which has been modelled in Creo parametric.
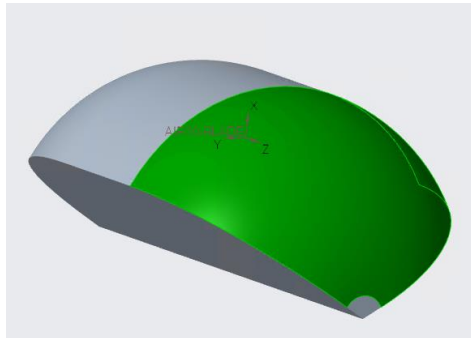
Figure 4-15 Hub

Figure 4-16 depicts the Creo model for blade and hub coupled together which will be assessed through Ansys software representing one third of the wind turbine.

Figure 4-16 Air 30 blade coupled with hub

The length of the hub is equal to 20 centimeters and both rounds in front and back is assigned 75 in Creo tools.

4.2.3. Control volume models (ICEM Ansys)

In order to analyze the behavior of the Air30 wind turbine, two domains have been modelled inside Creo parametric and then ICEM Ansys software used to mesh them. The first one is the pocket domain which contains the blade and hub is the rotating part and the second domain, the stationary one, representing the ambient to provide the inlet and outlet of the wind stream.

In Figure 4-17 the small domain (pocket) has been meshed with ICEM tools of Ansys software, containing the blade and hub. This domain has been discretized in unstructured mesh. The tetrahedra meshes has been assigned in a smaller scale for the blade and hub, in order to be more precise in these regions and bigger sizes for the remaining parts.

(a)   (b)
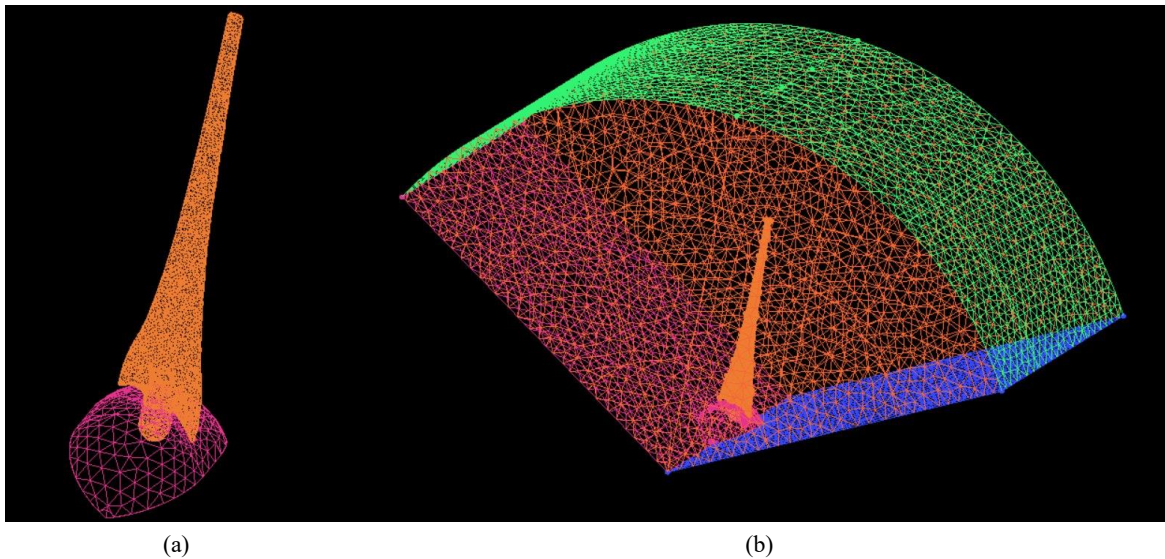
Figure 4-17 (a) Blade and hub model in ICEM, (b) Pocket model in ICEM

The characteristics of the pocket is written in Table 4-1.

Table 4-1 characteristics of the pocket model

Pocket length	80 cm
Hub length	20 cm
External Radius	1 m
Total elements	294511
Total nodes	49118

Figure 4-18 illustrates the bigger volume (Ambient) which has been formed in structured mesh. Structural mesh has been designed by creating a block and then cutting it into the different blocks corresponding to each section. Afterwards, each edge is associated with the corresponding point and curve in order to fit the geometry. The extrusion of this volume

isn't symmetrical, because the downstream section is much more important compared to the upstream part regarding the behavior of the air flow after the interaction with the blade; therefor, a longer control volume is needed. Moreover, in the vicinity of pocket zone, the density of mesh is higher, which results in much more accuracy in this zone as the flow becomes more unsteady.
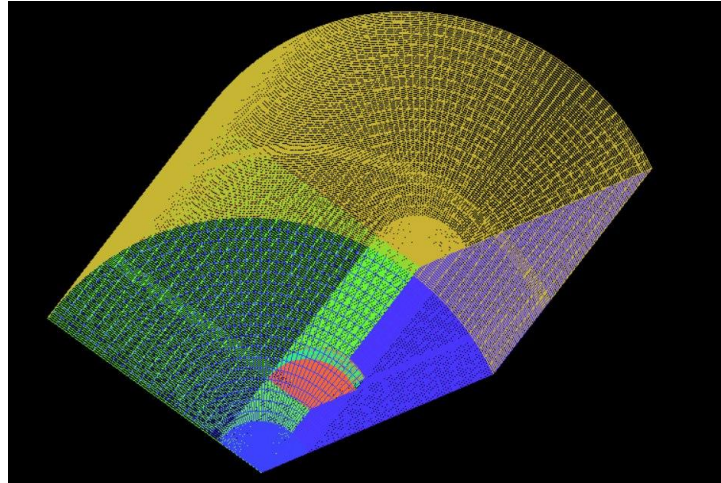

Figure 4-18 Ambient model in ICEM

Table 4-2 Characteristic of the ambient model

Length upstream	5 m
Length downstream	10 m
External Radius	5 m

The main advantages of this type of configurations are the better precision of the zone in the vicinity of the blade and hub and easier computational requirements needed by structured mesh in ambient section.

4.2.4. CFX setup (Ansys)

The following step after meshing the domains for ambient and the pocket is setting up the CFX, in order to define the stationary and rotating domains and also their corresponding boundary conditions. Reference pressure for both domains have to be defined here, by inserting 0 bar the relative pressure and absolute pressure would have the same meaning. Both fluid domains are defined as "Air at 25˚C", "Non buoyancy", and then "stationery" and "rotating" for ambient volume and pocket volume respectively.

Two domains can be connected through frozen rotor connection, which enables the software to model and partitioning the fluid into stationary and rotating sub-domain part. Additionally, frozen rotor connection enables the user to simulate the flow behavior inside a rotating domain without a need to model the whole cylinder. Therefore, this decreases the computational time and also without influencing the accuracy of the simulation. Finally, the interfaces have to be created to define each connection of the domains.

It has been noted that the control volumes are designed with only a 120˚angle, ignoring the complete rotation. This is mainly because the wind turbine maintains axial symmetry around its rotation axis, thus, this design strategy considers only one third of the control volume.

Once the imported parts are imported, after defining the rotating and stationary domains the main required boundary conditions have to be employed as follows:

1. The inflow surface of the large volume has been assigned to "Inlet". The normal speed of the flow is changed for each simulation in the range of 3 to 30 m/s.
2. The outflow surface of the large volume has been assigned to "Outlet". With the option of mass and momentum corresponding to "Entertainment" equal to value of 1 bar and "opening pressure" selected for pressure option and also "zero gradient" for the turbulence option.
3. The ceiling of the large volume (ambient) has been assigned to "Opening". With the opening pressure equal to 1 bar.
4. Blade and hub surfaces have been assigned to "Wall" considering "No slip wall" and "smooth surface".
5. Concerning the fluid model, the following assumptions have been employed:
    5.1 Heat transfer: "None"
    5.2 Turbulence: "Shear Stress Transport"
    5.3 Combustion: "None"
    5.4 Thermal radiation: "None"
6. Analysis type is set to "Steady State"
7. Maximum number of iterations to get convergence is equal to 1000.

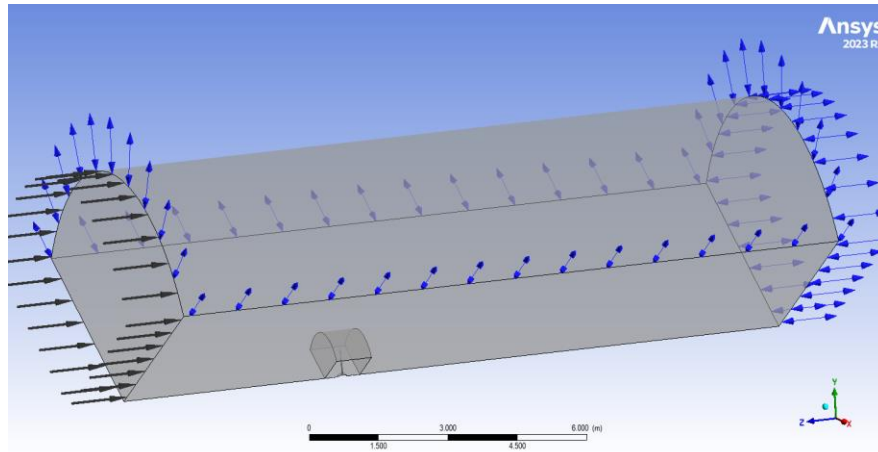In Figure 4-19 the boundary conditions required to run the simulation is illustrated.

Figure 4-19 CFX Setup of the wind turbine simulation

4.2.5. CFX Solver Manager (Ansys)

Once the domains and their corresponding boundary conditions and interfaces are ready, the system has to be run with the parameter assigning in solver control. The maximum number of iterations are assigned to 1000 to get the convergence.

4.2.6. CFD – post processing (Ansys)

The last step of each run is assessing and analyzing the behavior of the fluid and also the interaction characteristics with the blade and hub. CFD post enables the user to draw plans, stream lines, contours to depict the flow characteristics such as velocity, pressure, Mach number and other main factors and also it provides the researchers the ability of creating new variables and expressions based on their needs, Moreover, with this powerful tool the user can calculate the forces on 3 directions, torques which is really useful in terms of turbomachinery devices.

5. Results

5.1.   Room

5.1.1. Without internal wall

Figure 5-1 shows the flow behavior in the exhaust channel without the installation of the internal wall. It could be seen the flow would not be concentrated and homogenized and also the majority of it flow through the last silencers close to the wall.
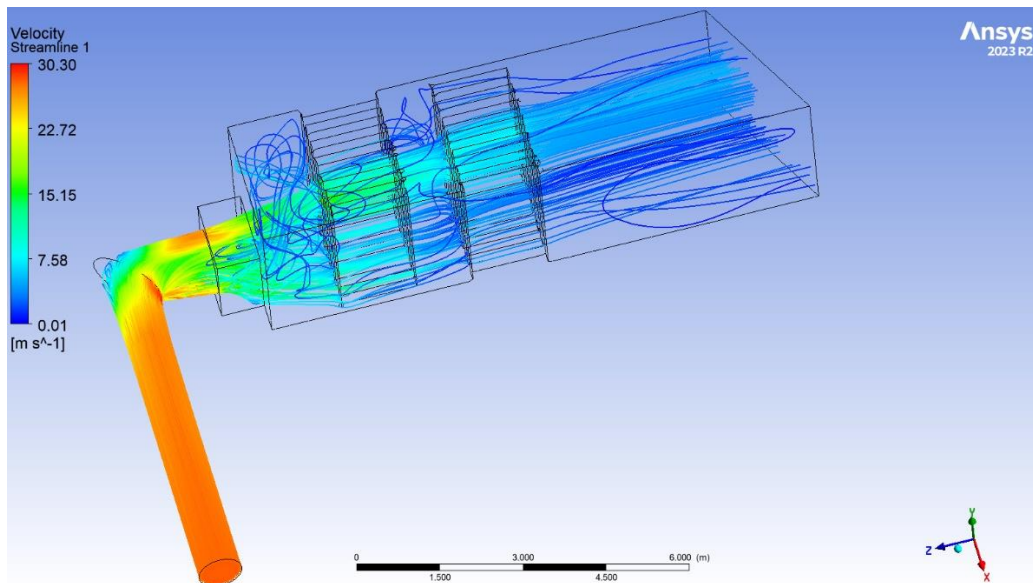
Figure 5-1 flow behavior in the exhaust channel without internal wall

Figure 5-2 illustrates the velocity values on the plane with only the beginning of 15 cm within the room. the right side of the room has the higher vales of velocity, and therefore its not applicable to install the wind turbine close to the wall to catch the higher velocities due to the size limit. So, one internal wall has to be installed with a hole in the middle of the wall to have a better flow in terms of velocity and also homogeneity.
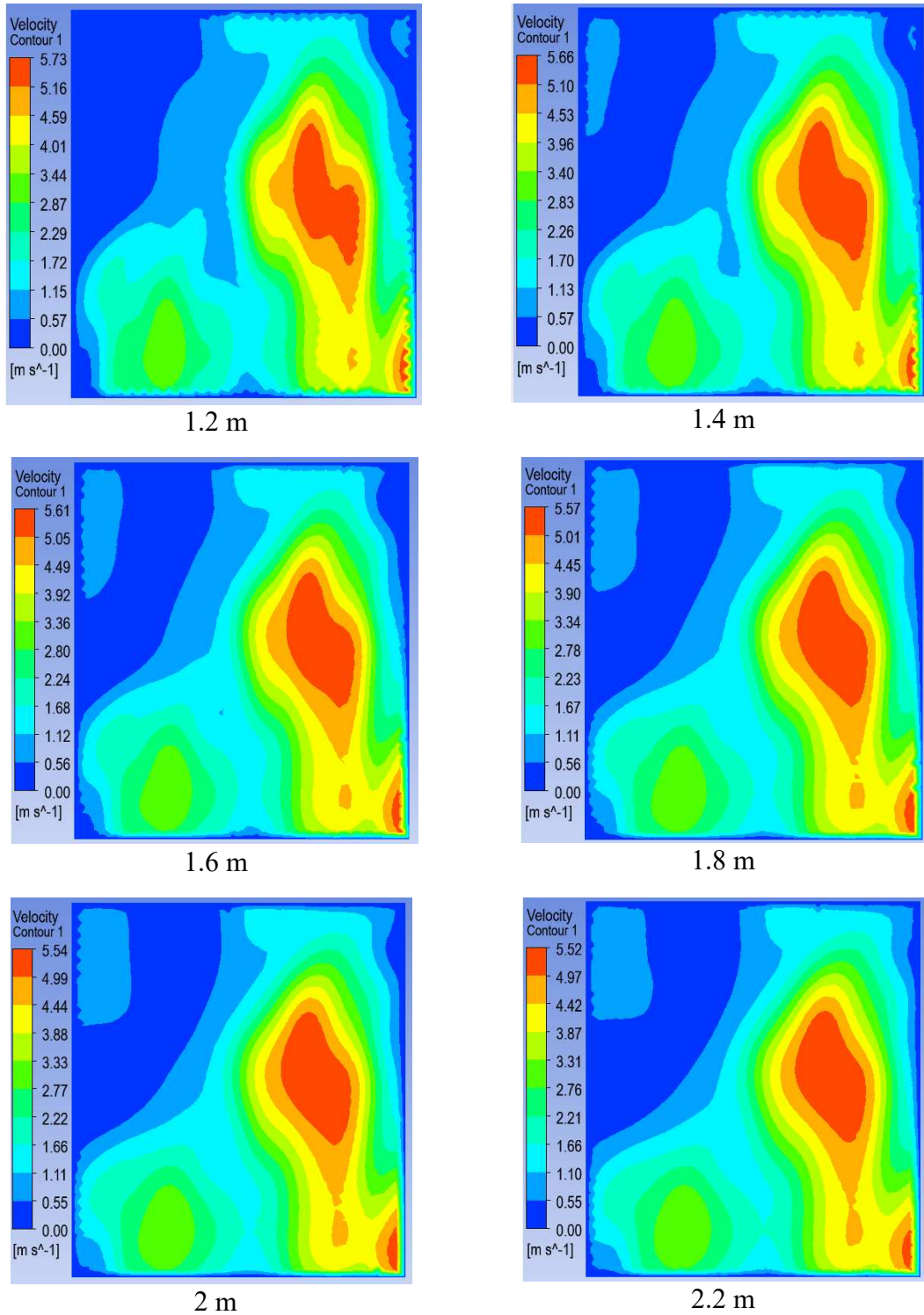
Results
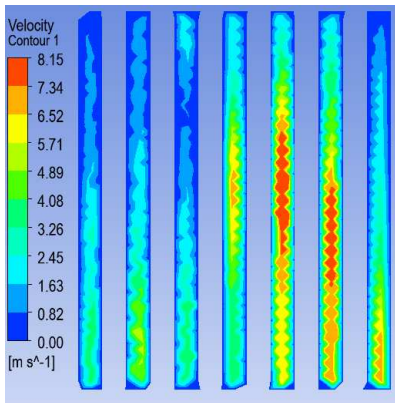
0 m
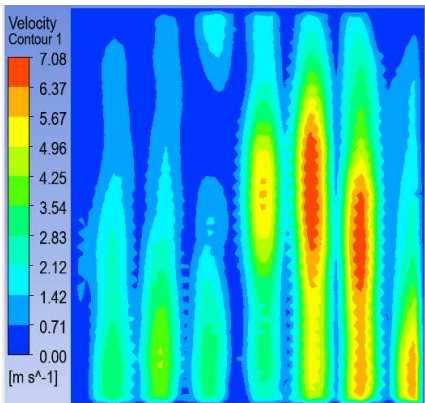
0.2 m
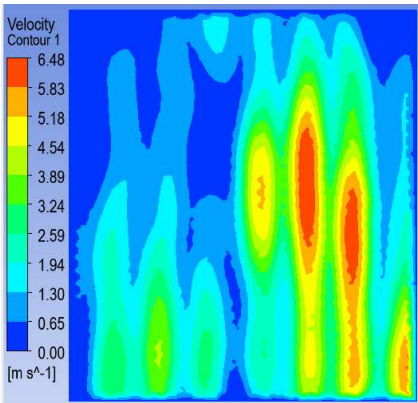
0.4 m

0.6 m

0.8 m

1 m

Results

1.2 m

1.4 m

1.6 m

1.8 m

2 m

2.2 m
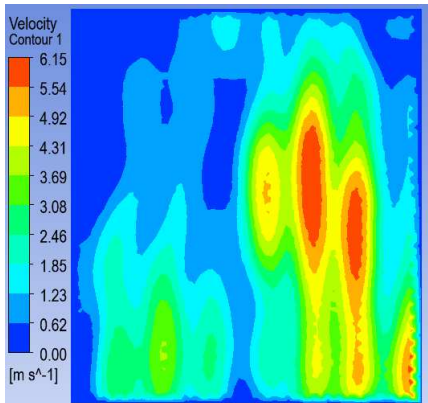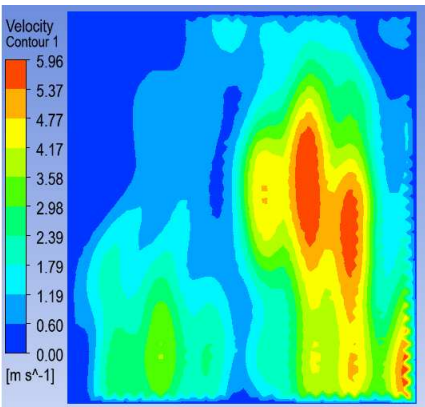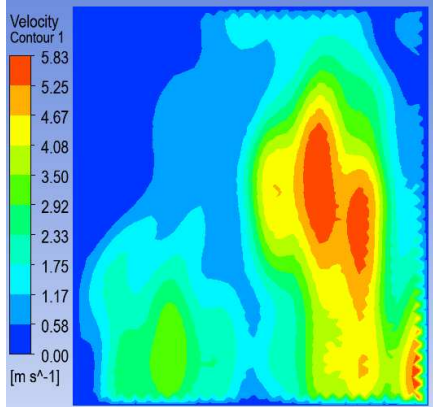
Figure 5-2 Velocity contour on the planes with different distances from the silencers within the room

Results

5.1.2. With internal wall

In Figure 5-3 the flow behavior inside the exhaust channel and the room has been illustrated. In which, it could be seen the effect of the hole in the internal wall after the silencers to make the flow more homogeneous.
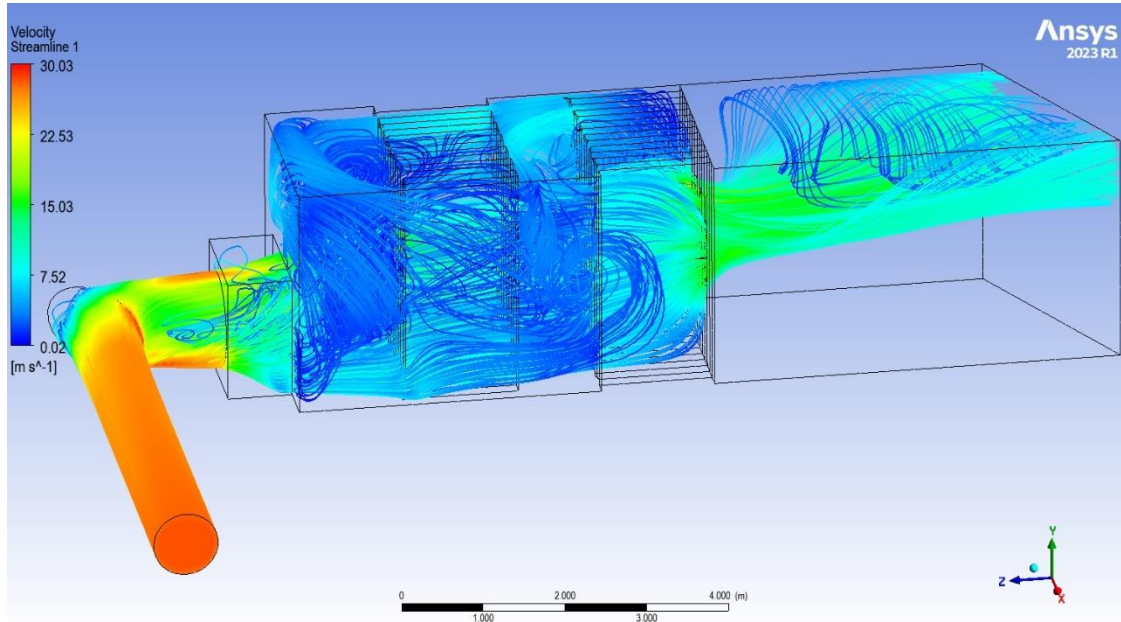

Figure 5-3 flow streamlines, inlet mass flow rate = 14.6 kg/s

By utilizing powerful tools in CFD, on each plane the velocities are derived and their Average velocities have been calculated.

Figure 5-5 illustrates the velocity contours on the planes with different distances (in the range between 0 between 2.2 meters) from the internal wall for the mass flow rate equal to 14.4 kg/s. the white ball represents the center of the hole. As it could be seen, the flow has an upward trend exiting the hole on the internal wall. The values of velocity for Figure 5-5 is depicted in Figure 5-4. The flow arrangement and its behavior is approximately the same for the other two mass flow rates with only one difference in velocity values.
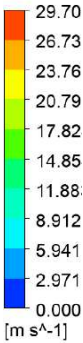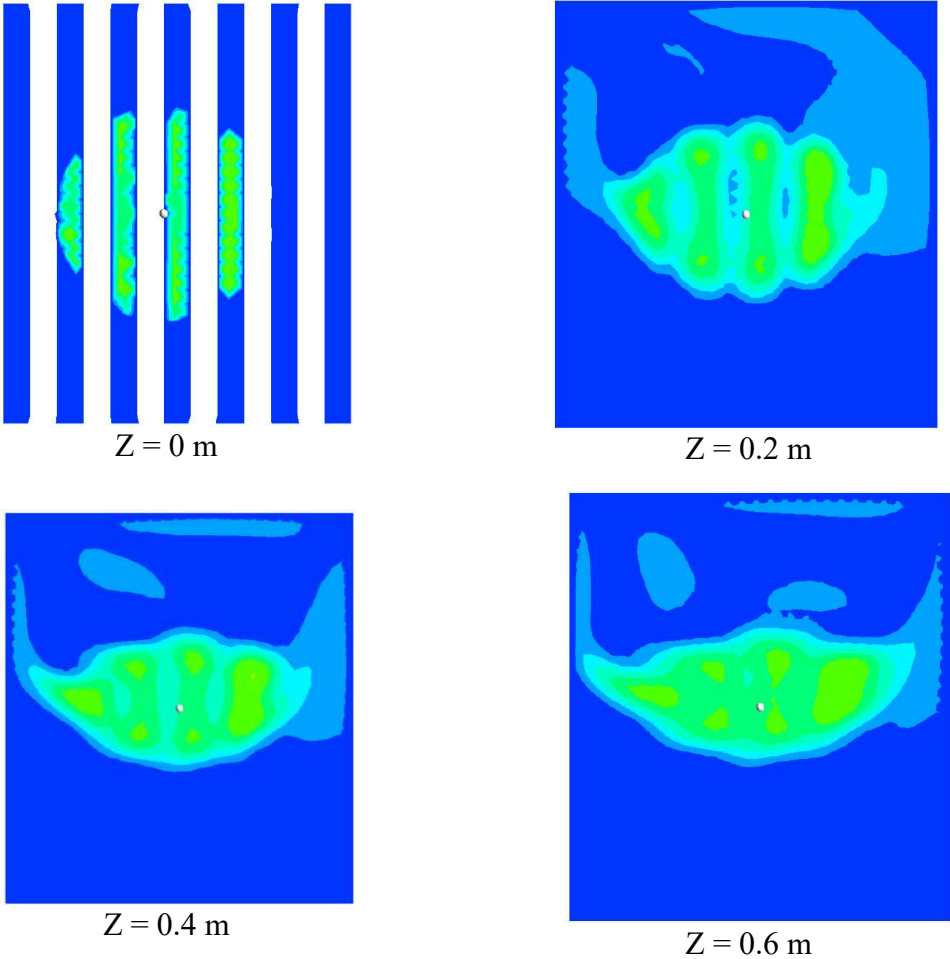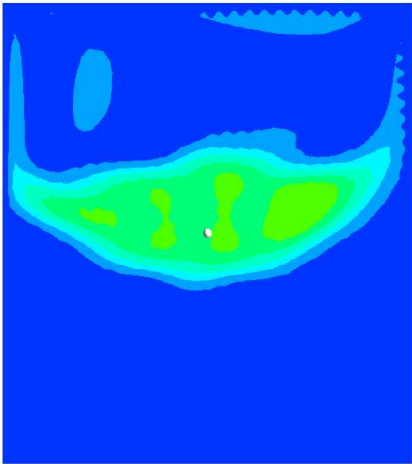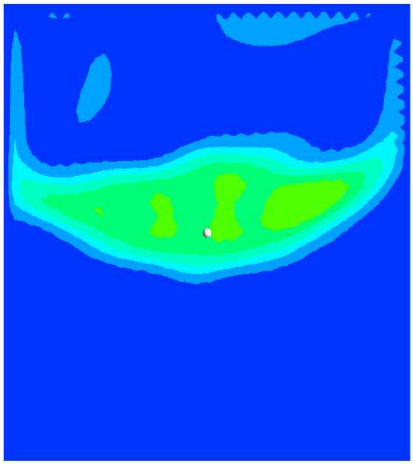
Results

Figure 5-4 Velocity legend values
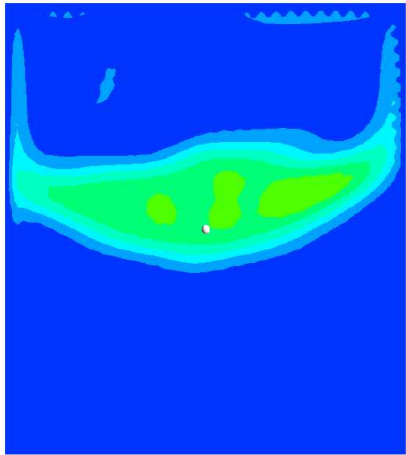

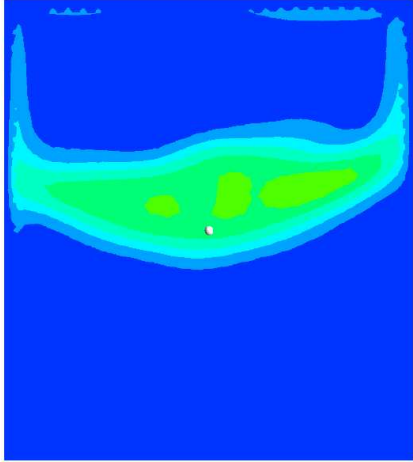Z = 0 m

Z = 0.2 m

Z = 0.4 m

Z = 0.6 m

Results

Z = 0.8 m

Z = 1 m

Z = 1.2 m
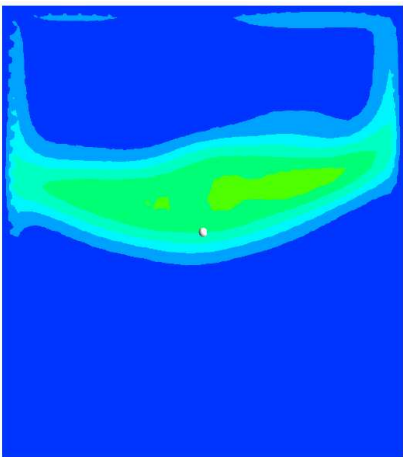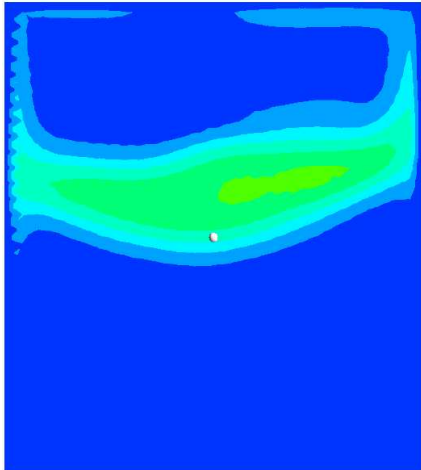

Z = 1.4 m

Z = 1.6 m

Z = 1.8 m

Results

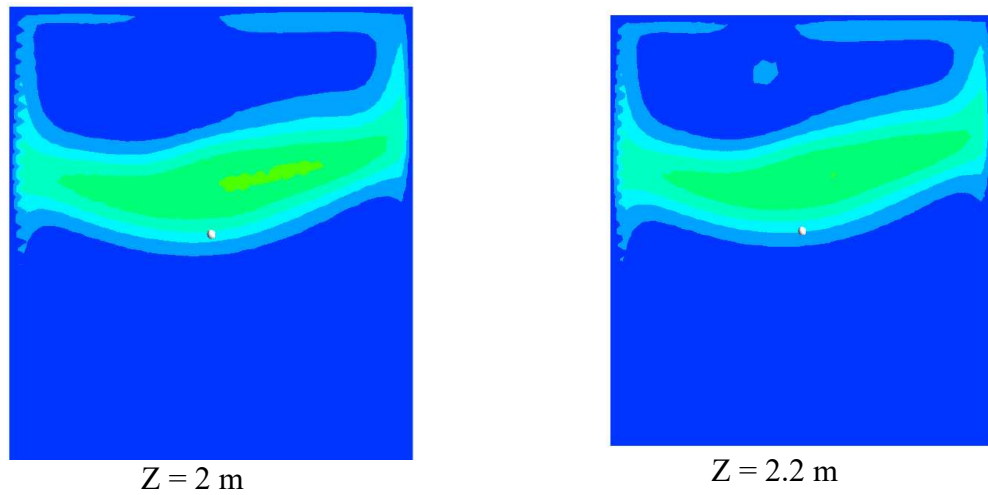Z = 2 m   Z = 2.2 m

Figure 5-5 Velocity contour on the planes with different distances within the room

In order to find the best location to install the wind turbine in the room, two parameters have been assessed including the average velocities and one index to define the homogeneity of the flow. As it has been explained before, within CFD post-processing, circular planes have been created. These planes share the same diameter as the hole within the internal wall and are spaced 20 cm apart. The arrangement of the circular planes is illustrated in Figure 5-6.
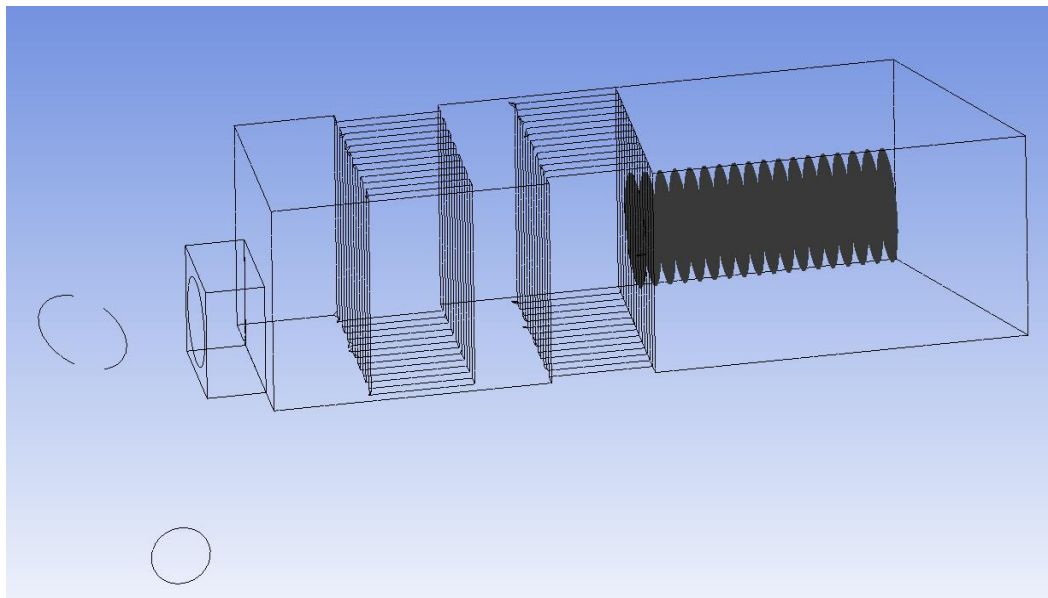

Figure 5-6 Circular planes defined in CFD-post

To assess the flow homogeneity, the coefficient of variation is introduced. The coefficient of variation is a statical measure that quantifies the relative variability of the dataset. In this

work, this variable has been defined using the equation 28. A higher Coefficient of variation indicates greater relative variability within the dataset, conversely, a lower value suggests that the data are more homogenous or tightly clustered around the mean value.

$$CV = \frac{Standard\ deviation\ of\ the\ velocities\ on\ each\ plane}{Average\ value\ of\ the\ velocities\ on\ each\ plane} \qquad (5.1)$$

The model has been analyzed with three different mass flow rates: 14.6, 11.3, 8kg/s. These values of inlet are derived from the outlet of the radial compressor in the department of mechanical engineering.

Figure 5-7 illustrates the average velocity on the circular planes versus the distance from the internal wall for three different mass flow rates as inlet. The more the distance from the wall the lower the velocities could be figured out.
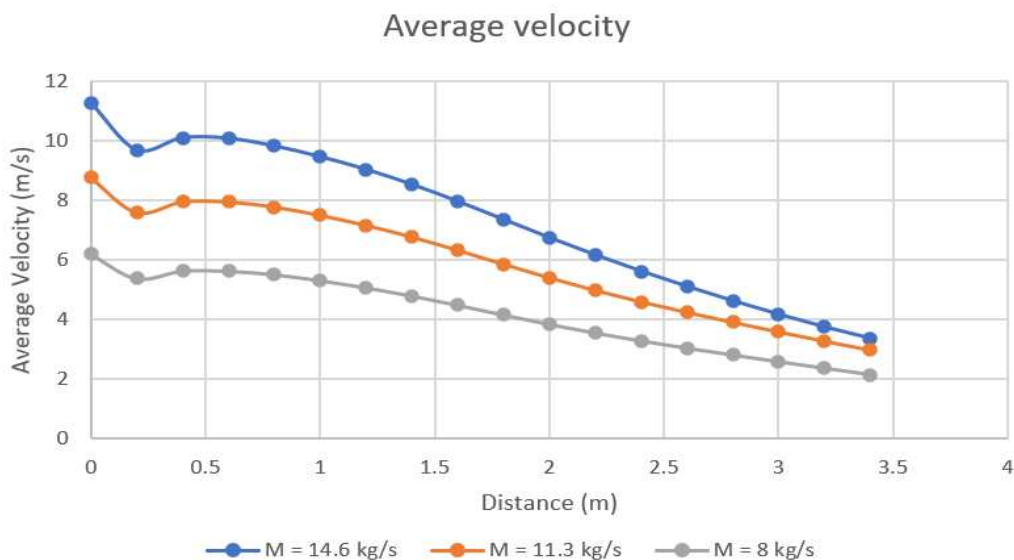

Figure 5-7 Average velocity versus distance from the internal wall

In assessing the homogeneity of flow, Figure 5-8 illustrates the relationship between the Coefficient of Variation and the distance from the wall. Notably, observations indicate that within a distance of less than 1 meter from the wall, there is a diminished relative variability in flow across the circular plane. Additionally, within the larger distances from the wall, the higher variation of the flow speeds on the corresponding circular plane could be seen.
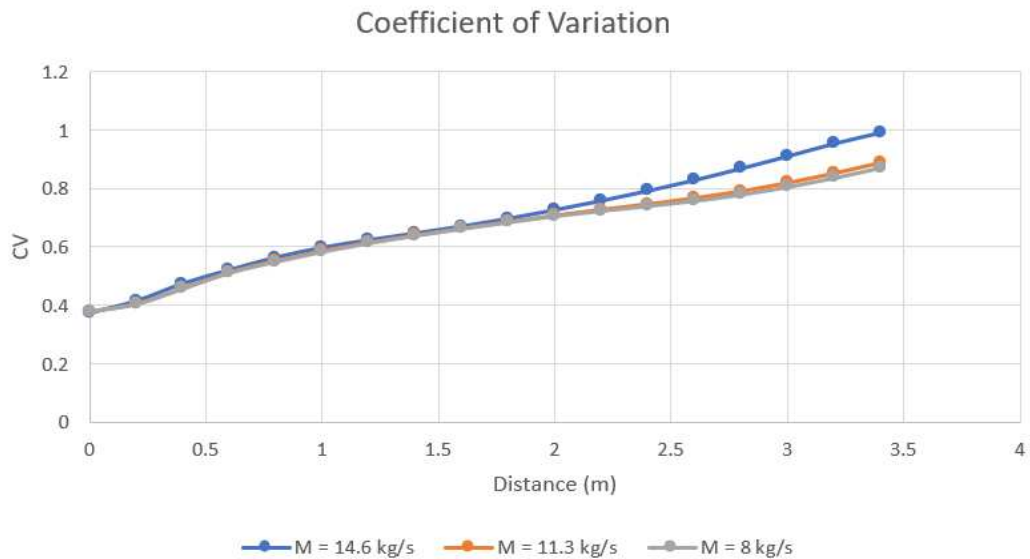
Figure 5-8 Coefficient of variation versus distance from the internal wall

5.1.3. Adding a honey comb

In section 4.1.4, the characteristics of the honeycomb structure has been well defined, evaluating three different porosities with the aim of achieving flow homogeneity. In this section, the average velocities on the same planes defined in the CFD post-processing section has been analyzed. In on other words, each data point on these graphs represents the average velocity along the planes—from the internal wall to the outlet—within the room. additionally, data set of the coefficient of variation of the velocities on each plane is also illustrated for each different porosity.

5.1.3.1. Without Porosity

Figure 5-9 illustrates the avergae velocity and coefficient of variation of the flow as a function of the distance from the internal wall with assuming zero percent porosity for the poros domain.

Results
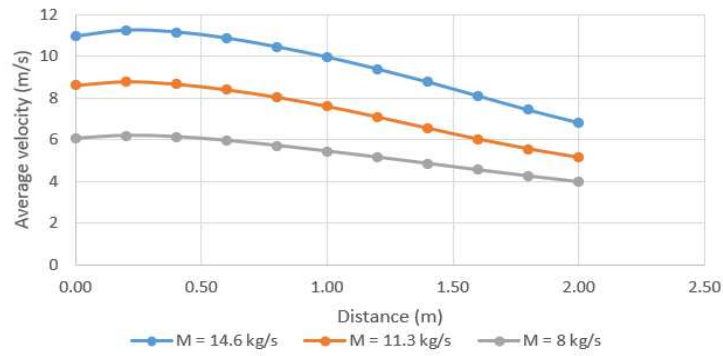
(a)

(b)

Figure 5-9 honey comb without porous domain; (a) average velocity versus distance,
(b) Coefficient of variation versus distance

5.1.3.2. Porosity = 40 %

Figure 5-10 illustrates the avergae velocity and coefficient of variation of the flow as a function of the distance from the internal wall with assuming 40 percent porosity for the poros domain.

Results

(a)

(b)

Figure 5-10 honey comb with 40% porous domain; (a) average velocity versus distance, (b) Coefficient of variation versus distance
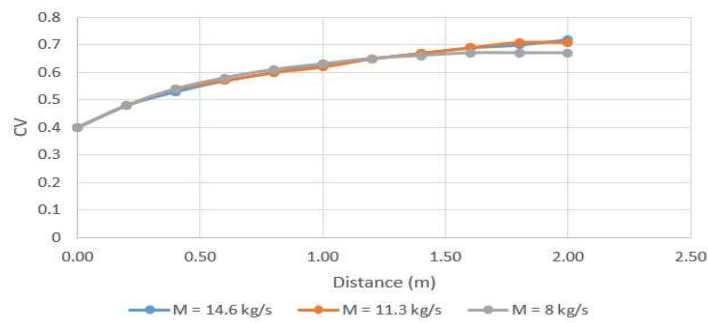
5.1.3.3.   Porosity = 70%

Figure 5-11 illustrates the avergae velocity and coefficient of variation of the flow as a function of the distance from the internal wall with assuming 70 percent porosity for the poros domain.

(a)
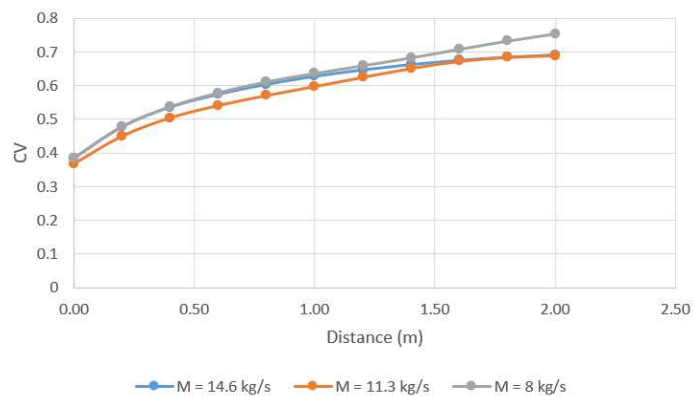
(b)

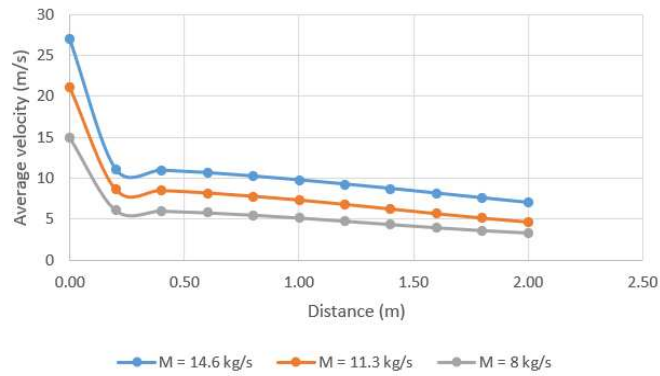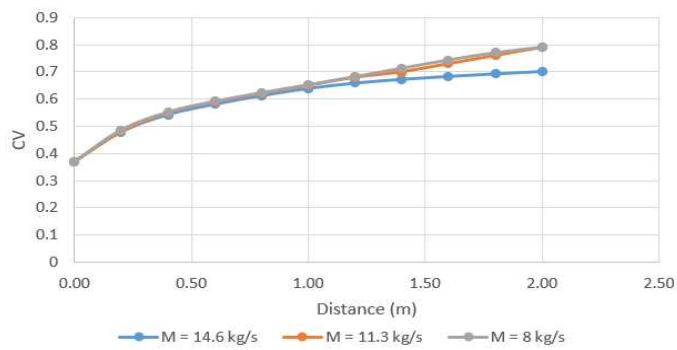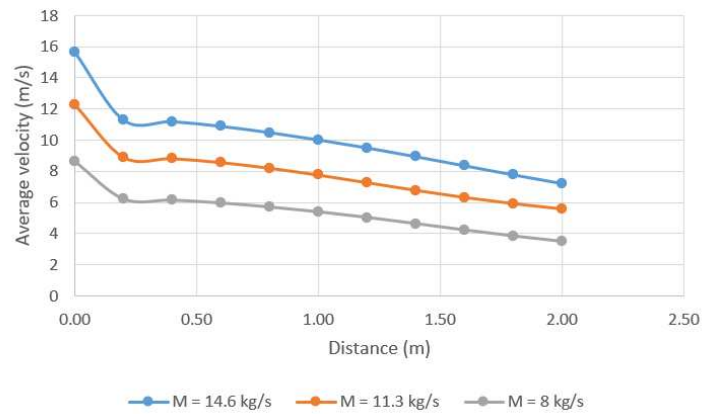Figure 5-11 honey comb with 70% porous domain; (a) average velocity versus distance, (b) Coefficient of variation versus distance

5.1.4. The impact of adding a cylindrical honeycomb

Figure 5-12 illustrates the influence of adding a cylindrical honey comb installed on the internal wall on the average velocities of each plane within the room and also the coefficient of variation, which stands for the homogeneity index of the flow.

It could be figured out, in the first 50-centimeter distance from the internal wall (30-centimeter from the honeycomb), the addition of honey comb results in increasing approximately 9 to 15% of the velocity but at the same time more than 10% of coefficient of variation.

Results

Effect on average velocity (%)   Effect on coefficient of variation (%)
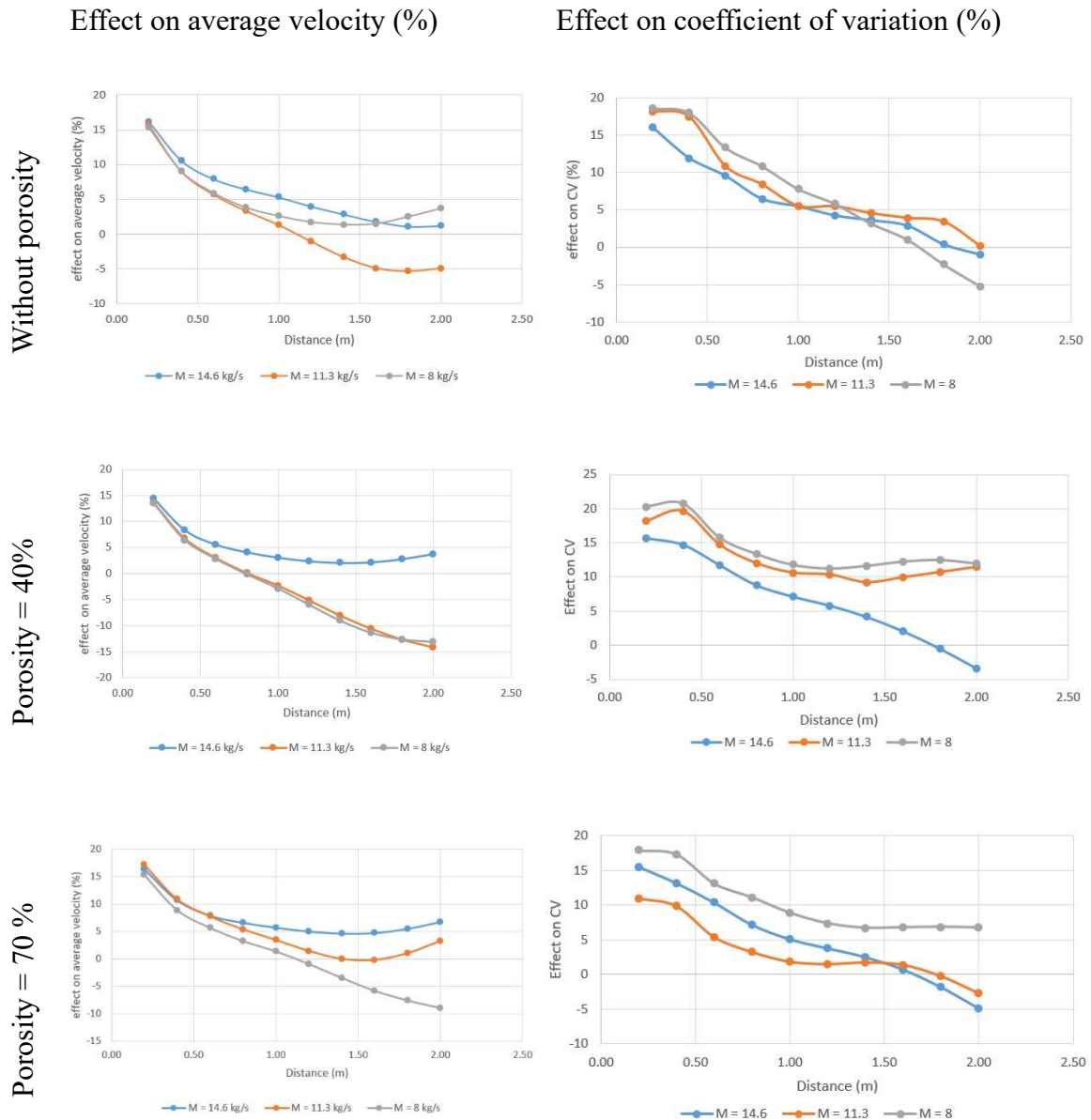
Figure 5-12 Effect of adding a honeycomb

5.1.5. The impact of porosity

Figure 5-13 illustrates the influence of three distinct conditions on the porosity values of the second segment of the honeycomb structure. Therefore, it is obvious, that the impact of porosity can be deemed negligible. The main reason of the negligible effect of porosity on the flow is that the flow is particularly dependent upon the mass flow rate. In other words, in the same mass flow rates, 2 cm porous domain of the honey comb exhibit minimal changes on both flow velocity and its homogeneity.

Results

The first 20-cm distance in Figure 5-13, shows the flow behavior inside the honeycomb in which, considerable increase of flow velocity is due to the pressure drop in that part. This increment of velocity remains immediately consistent upon exiting the honey comb regardless of different values of porosity.

Effect on average velocity (%)   Effect on Coefficient of variation (%)

Figure 5-13 Effect of porous domain

5.2. Evaluation of wind turbine performance

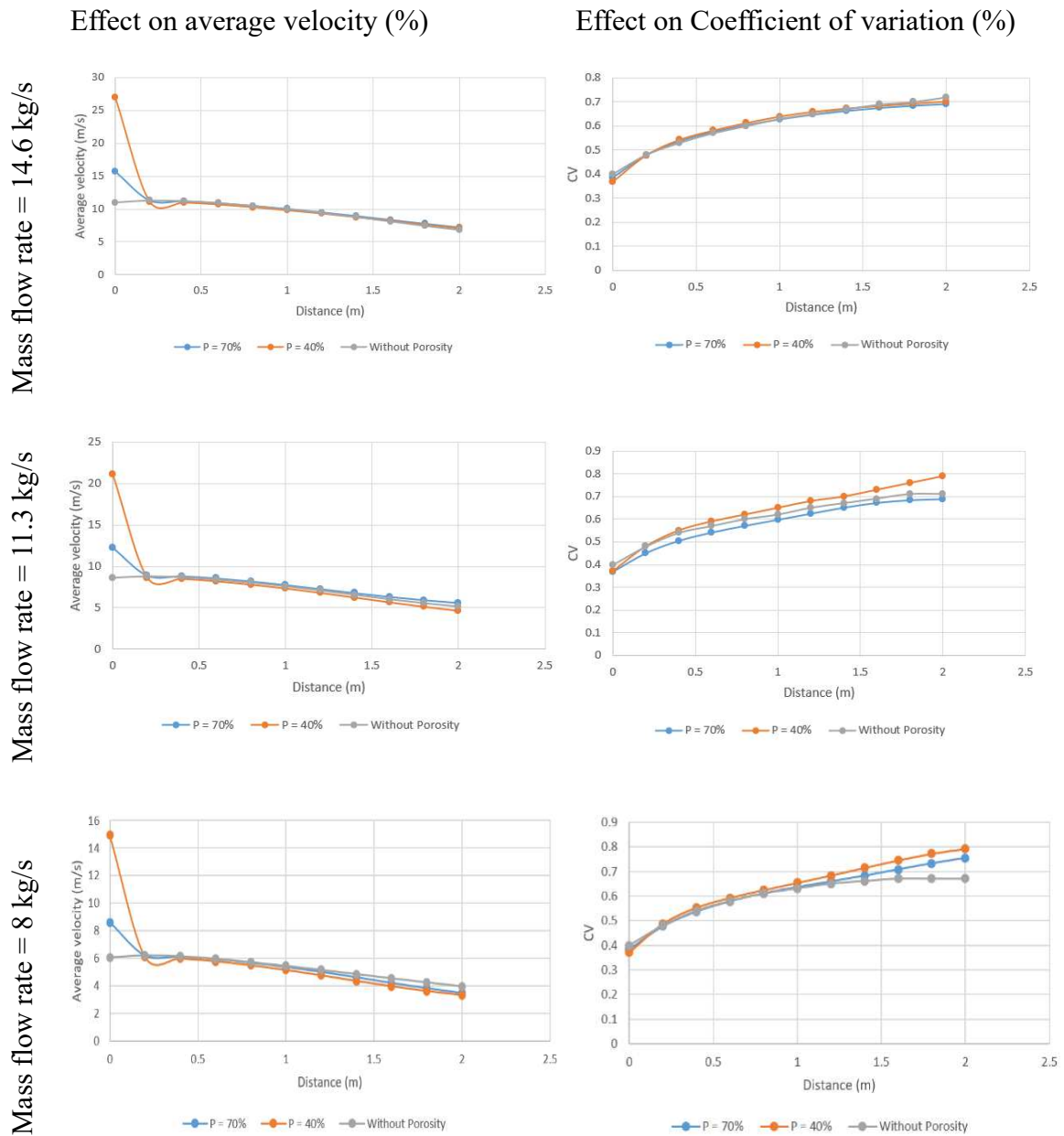As it has previously been explained in section 4.2.6, CFD post processing enables the user to calculate the values of the torque on the blade by defining torque variable within the axis of the rotation (in this study is Z axis). Given that only one third of the turbine is modeled, it's reasonable to assume that the total torque would be tripled accordingly. Power can be calculate using the equation below:

$$P = T.\omega \tag{5.2}$$

Where T is torque and W is the angular velocity of the wind turbine equal to 840 revolution per minute (87.96 rad/s).

Table 5-1 Torque and Power output in different wind speeds condition

Wind speed (m/s)	Torque (N.m)	Power (Watt)
4	-0.3771	0
6	0.04023	3.54
8	0.3582	31.51
10	0.7251	63.78
12	1.0218	89.88
16	1.4151	124.48

Figure 5-14 depicts the extracted power in different wind speeds conditions. It could be seen that the minimum required wind speed for the wind turbine to generate torque is approximately equal to 4.8 m/s.
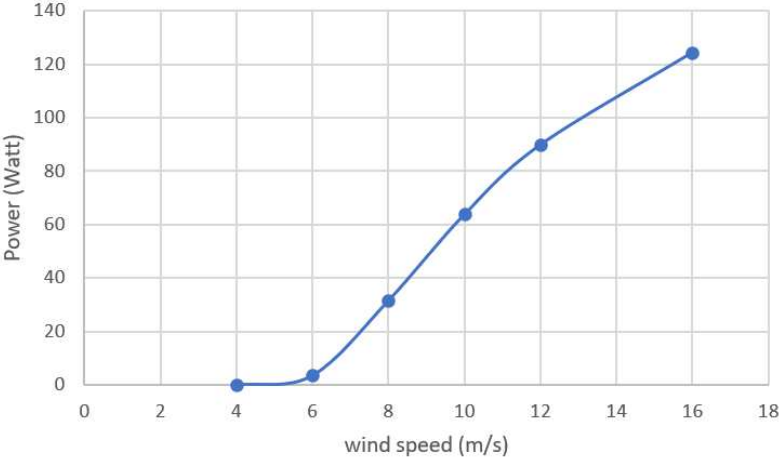
Results

Figure 5-14 Power output versus wind speed

6. Conclusion

Based on the design and assessment efforts in this work study, it can be concluded that the it would be better to install an internal wall with a hole in the center of it to make the flow more homogenize. Without the internal wall, it's not reasonable to install the wind turbine as the flow flowing through the last silencers which make the installation impossible due to the size of the wind turbine.

Installation of the honey comb will improve the homogeneity of the flow and also increase the velocity of the flow up to 15% which is are the crucial factors to the extract power of the wind turbine. Additionally, after the assessment of the different honey combs structure with in terms of porosity, it has been figured out that the impact of the porosity can be considered negligible.

At the end, the evaluation of air 30 turbine which has been accomplished by one third of the wind turbine simulated and the power curve versus different velocities shows the small cut-in speed around 5 m/s which is the main advantages of the small wind turbines.

7. References

[1]   V. Masson-Delmotte, P. Zhai, A. Pirani et al. (eds.), "Climate Change 2021: The Physical Science Basis. Contribution of Working Group I to the Sixth Assessment Report of the Intergovernmental Panel on Climate Change," *IPCC, 2021,* 2021.

[2]   Nguyen, "A critical review on potential and current status of wind energy in Vietnam," *Renewable and Sustainable Energy Reviews,* vol. 43, pp. 440-448, 2015, doi: https://doi.org/10.1016/j.rser.2014.11.060.

[3]   I. (2023), "CO2 Emissions in 2022," 2023. [Online]. Available: https://www.iea.org/reports/co2-emissions-in-2022

[4]   I. E. Agency. "Net renewable electricity capacity additions by technology, 2017-2024." https://www.iea.org/reports/renewable-energy-market-update-june-2023 (accessed 22 Dec 2023.

[5]   S. Raafat and R. Hussein, "Power Maximization and Control of Variable-Speed Wind Turbine System Using Extremum Seeking," *Journal of Power and Energy Engineering,* vol. 06, pp. 51-69, 01 2018, doi: 10.4236/jpee.2018.61005.

[6]   S. Eriksson, H. Bernhoff, and M. Leijon, "Evaluation of different turbine conceps for wind power," *Renewable and Sustainable Energy Reviews,* vol. 12, pp. 1419-1434, 06 2008, doi: 10.1016/j.rser.2006.05.017.

[7]   J. Akwa, H. Vielmo, and A. Petry, "A review on the performance of Savonius wind turbines," *Renewable and Sustainable Energy Reviews,* vol. 16, pp. 3054–3064, 06 2012, doi: 10.1016/j.rser.2012.02.056.

[8]   R. Kishore, s. J. Priya, and C. Stewart, *Wind Energy Harvesting: Micro-to-Small Scale Turbines*. 2018.

[9]   I. Mazharul, S. K. T. David, and F. Amir, "Aerodynamic models for Darrieus-type straight-bladed vertical axis wind turbines," *Renewable and Sustainable Energy Reviews,* vol. 12, no. 4, pp. 1087-1109, 2008, doi: https://doi.org/10.1016/j.rser.2006.10.023.

[10]   R. Dominy, P. Lunt, A. Bickerdyke, and J. Dominy, "Self-starting capability of a Darrieus turbine," *Proceedings of the Institution of Mechanical Engineers Part A Journal of Power and Energy,* vol. 221, 02 2007, doi: 10.1243/09576509JPE340.

[11]   H. Hirahara, M. Hossain, M. Kawahashi, and Y. Nonomura, "Testing basic performance of a very small wind turbine designed for multi-purposes," *Renewable Energy,* pp. 1279-1297, 01 2005, doi: 10.1016/j.renene.2004.10.009.

[12]   N. Ahmed, B. S. Yilbas, and M. O. Budair, "Computational study into the flow field developed around a cascade of NACA 0012 airfoils," *Computer Methods in Applied Mechanics and Engineering,* vol. 167, no. 1, pp. 17-32, 1998, doi: https://doi.org/10.1016/S0045-7825(98)00104-2.

[13]   R. Lanzafame and M. Messina, "Power curve control in micro wind turbine design," *Energy,* vol. 35, no. 2, pp. 556-561, 2010, doi: https://doi.org/10.1016/j.energy.2009.10.025.

[14]   R. Kishore, T. Coudron, and s. J. Priya, "Small-scale wind energy portable turbine (SWEPT)," *Journal of Wind Engineering and Industrial Aerodynamics,* vol. 116, pp. 21–31, 05 2013, doi: 10.1016/j.jweia.2013.01.010.

[15]   O. Ozgener and L. Ozgener, "Exergy and reliability analysis of wind turbine systems: A case study," *Renewable and Sustainable Energy Reviews,* vol. 11, pp. 1811-1826, 10 2007, doi: 10.1016/j.rser.2006.03.004.

[16]   P. w. power. Prismus wind power. https://www.primuswindpower.com/ (accessed 29

December 2023, 2023).

[17]   R. Energy. "mirco wind tubines." https://www.ryse.energy/air-40-turbine/ (accessed 1 jan, 2024).

[18]   S. Ani, H. Polinder, and J. A. Ferreira, "Low cost axial flux PM generator for small wind turbines," presented at the 2012 IEEE Energy Conversion Congress and Exposition, ECCE 2012, 09, 2012.

[19]   D. Wood, "Small wind turbines : analysis, design, and application David Wood.," ed. New York: Springer, 2011.

[20]   M. O. L. Hansen, *"Aerodynamics of Wind Turbines: second edition"*, "2" ed. Earthscan, 2008.

[21]   O. Apata and D. T. O. Oyedokun, "An overview of control techniques for wind turbine systems," *Scientific African,* vol. 10, p. e00566, 2020, doi: https://doi.org/10.1016/j.sciaf.2020.e00566.

[22]   S.-L. Tai, Berg, L. K., Krishnamurthy, R., Newsom, R., and Kirincich, A, "Validation of turbulence intensity as simulated by the Weather Research and Forecasting model off the US northeast coast, Wind Energ, Sci., 8, 433–448." [Online]. Available: https://doi.org/10.5194/wes-8-433-2023, 2023.

[23]   L. J. a. C. Andrew. "How turbulence can impact power performance." https://www.wind-watch.org/documents/how-turbulence-can-impact-power-performance/#:~:text=The%20turbulence%20of%20the%20inflow,very%20large%20impacts%20on%20loads. (accessed 2 jan, 2024).

[24]   S. Zergane and A. Smaili, "Effect of Turbulence on Wind Turbine Farm Power Production," Singapore, 2021: Springer Singapore, in Advances in Green Energies and Materials Technology, pp. 393-400.

[25]   S. Lee, M. Churchfield, P. Moriarty, J. Jonkman, and J. Michalakes, "Atmospheric and Wake Turbulence Impacts on Wind Turbine Fatigue Loading: Preprint," 01 2012, doi: 10.2514/6.2012-540.

[26]   T. Miguel and S. Fangjun, "Experimental study of turbulence intensity influence on wind turbine performance and wake recovery in a low-speed wind tunnel," *Renewable Energy,* vol. 109, pp. 363-371, 2017, doi: https://doi.org/10.1016/j.renene.2017.03.034.

[27]   A. Al-Abadi, Y. J. Kim, E. Ö, and A. Delgado, "Turbulence Impact on Wind Turbines: Experimental Investigations on a Wind Turbine Model," *Journal of Physics: Conference Series,* vol. 753, no. 3, p. 032046, sep 2016, doi: 10.1088/1742-6596/753/3/032046.

[28]   W. Lubitz, "Impact of Ambient Turbulence on Performance of a Small Wind Turbine," *Renewable Energy,* vol. 61, 01 2014, doi: 10.1016/j.renene.2012.08.015.

[29]   I. U. Mitsumasa Iino, "Effect of High Turbulence Intensity on Micro Wind Turbine Performance " *Journal of Multidisciplinary Engineering Science and Technology (JMEST,* vol. Vol. 6 Issue 11, 2019.

[30]   C. P. Luisa, B. Massimiliano, and R. Maria Pia, "Experimental power curve of small-size wind turbines in turbulent urban environment," *Applied Energy,* vol. 154, pp. 112-121, 2015, doi: https://doi.org/10.1016/j.apenergy.2015.04.117.

[31]   W. D. a. C. Musial, D E, "Influence of Reynolds number on performance modeling of horizontal axis wind rotors," vol. 110:2, 1988, doi: 10.1115/1.3268244.

[32]   C. S. A. Ravi Anant Kishore, Shashank Priya, in *Wind energy harvesting : micro- to small-scale turbines*, (De Gruyter textbook. Berlin: De Gruyter, 2018.